EBioMedicine 64 (2021) 103196

Contents lists available at ScienceDirect

EBioMedicine

journal homepage: www.elsevier.com/locate/ebiom

Research paper

# Repopulation of decellularised articular cartilage by laser-based matrix engraving

S. Nürnberger[a,b,c,*], C. Schneider[b,c], C. Keibl[b], B. Schädl[b,c,e], P. Heimel[b,c,e], X. Monforte[d], A.H. Teuschl[c,d], M. Nalbach[f], P.J. Thurner[f], J. Grillari[b,c,g], H. Redl[b,c], S. Wolbank[b,c]

[a] Department of Orthopedics and Trauma-Surgery, Division of Trauma-Surgery, Medical University of Vienna, Vienna, Austria
[b] Ludwig Boltzmann Institute for Experimental and Clinical Traumatology in AUVA Trauma Research Center, Vienna, Austria
[c] Austrian Cluster for Tissue Regeneration, Vienna, Austria
[d] Department Life Science Engineering, University of Applied Sciences Technikum Wien, Vienna, Austria
[e] University Clinic of Dentistry, Medical University of Vienna, Vienna, Austria
[f] Institute of Lightweight Design and Structural Biomechanics, TU Wien, Vienna, Austria
[g] Department of Biotechnology, BOKU-University of Natural Resources and Life Sciences Vienna, Austria

ARTICLE INFO

*Article History:*
Received 31 August 2020
Revised 25 November 2020
Accepted 15 December 2020
Available online 19 January 2021

*Keywords:*
Cartilage regeneration
Decellularisation
Laser engraving
Repopulation
Mechanical testing
Ectopic animal model

ABSTRACT

*Background:* In spite of advances in the treatment of cartilage defects using cell and scaffold-based therapeutic strategies, the long-term outcome is still not satisfying since clinical scores decline years after treatment. Scaffold materials currently used in clinical settings have shown limitations in providing suitable biomechanical properties and an authentic and protective environment for regenerative cells. To tackle this problem, we developed a scaffold material based on decellularised human articular cartilage.

*Methods:* Human articular cartilage matrix was engraved using a $CO_2$ laser and treated for decellularisation and glycosaminoglycan removal. Characterisation of the resulting scaffold was performed via mechanical testing, DNA and GAG quantification and *in vitro* cultivation with adipose-derived stromal cells (ASC). Cell vitality, adhesion and chondrogenic differentiation were assessed. An ectopic, unloaded mouse model was used for the assessment of the *in vivo* performance of the scaffold in combination with ASC and human as well as bovine chondrocytes. The novel scaffold was compared to a commercial collagen type I/III scaffold.

*Findings:* Crossed line engravings of the matrix allowed for a most regular and ubiquitous distribution of cells and chemical as well as enzymatic matrix treatment was performed to increase cell adhesion. The biomechanical characteristics of this novel scaffold that we term CartiScaff were found to be superior to those of commercially available materials. Neo-tissue was integrated excellently into the scaffold matrix and new collagen fibres were guided by the laser incisions towards a vertical alignment, a typical feature of native cartilage important for nutrition and biomechanics. In an ectopic, unloaded *in vivo* model, chondrocytes and mesenchymal stromal cells differentiated within the incisions despite the lack of growth factors and load, indicating a strong chondrogenic microenvironment within the scaffold incisions. Cells, most noticeably bone marrow-derived cells, were able to repopulate the empty chondrocyte lacunae inside the scaffold matrix.

*Interpretation:* Due to the better load-bearing, its chondrogenic effect and the ability to guide matrix-deposition, CartiScaff is a promising biomaterial to accelerate rehabilitation and to improve long term clinical success of cartilage defect treatment.

*Funding:* Austrian Research Promotion Agency FFG ("CartiScaff" #842455), Lorenz Böhler Fonds (16/13), City of Vienna Competence Team Project Signaltissue (MA23, #18-08)



## 1. Introduction

Large articular cartilage defects require biomaterial-supported cell therapy to deliver and distribute regenerative cells at the site of cartilage loss and to initiate *in vivo* regeneration. Amongst a variety of strategies using biomaterials with pre-cultivated or intraoperatively

* Corresponding author at: Department of Orthopedics and Trauma-Surgery, Division of Trauma-Surgery, Medical University of Vienna, Vienna, Austria
*E-mail address:* sylvia.nuernberger@meduniwien.ac.at (S. Nürnberger).

https://doi.org/10.1016/j.ebiom.2020.103196

**Research context**

*Evidence before this study*

Biomaterial-supported cartilage defect treatment is the gold standard of large chondral defect regeneration and leads to improvement of clinical symptoms within the first postoperative year. However, the recovery is often incomplete and reoperation was reported in up to 20% of the patients. In addition, long-term studies reveal late deterioration of clinical parameters (patient-reported outcome measures). The rare biopsies available from transplanted areas show structural differences of the formed tissue in comparison with native cartilage. A random alignment of collagen is visible in fibrous tissues, which might lead to secondary degradation due to insufficient biomechanics, fluid flow and nutrition. Since matrix alignment is guided by scaffolding biomaterials and materials currently in clinical use feature a random alignment, scaffold architecture could be the reasons for inappropriate repair tissue formation.

*Added value of this study*

To our knowledge, this is the first study showing $CO_2$ laser engraving of cartilage in this high accuracy, depth and narrow spacing, considering also beam damage and strategies to avoid it, and furthermore achieving a clear chondro-supportive effect.

The decellularised cartilage scaffold developed in this study provides a better load-bearing capacity than commercially available materials, guides accurate matrix deposition and provides a cartilage-like architecture with authentic zonation including the superficial zone. In addition, it supports chondrogenesis, especially in the depth of the laser-engraved incisions.

*Implications of all the available evidence*

CartiScaff is a promising biomaterial to accelerate rehabilitation due to earlier load-bearing and chondrogenic properties and may have the potential to improve long term clinical success in the treatment of cartilage defects.

harvested chondrocytes, stem cells or progenitor cell populations, the matrix-associated chondrocyte transplantation (MACT or MACI) is the method established the longest with follow-up periods of up to 20 years [1-3]. Indeed, this treatment strategy leads successfully to improvement of symptoms in most patients [2,4,5]. However, in long-term observations, graft failures and reoperations in up to twenty percent of the patients, occurring either early after implantation or after several years, were reported [6-11]. Early graft failures often result from insufficient rehabilitation or traumatic events after implantation [1,12] while later deterioration may take place after several years, even if clinical parameters had indicated a good performance in the early phase [4,6,7]. The rare biopsies available from transplanted areas, harvested in the course of clinically indicated reoperations or as experimental endoscopic biopsies, reveal incompletely masked hyaline cartilage with random collagen alignment [13-15] and the formation of fibrocartilage in a majority of defects [16,17]. This repair tissue differs from native hyaline cartilage, which features completely masked collagen fibres by incorporation of glycosaminoglycans (GAG) and a complex collagen architecture with generally vertical alignment in deeper regions, with fibrils bending towards the upper regions and being horizontally aligned at the surface [18,19]. This particular structure is crucial for biomechanics, fluid flow and nutrition [20-22], suggesting that randomly organised regenerated matrix does not fulfil the requirements in the long run and probably leads to secondary degradation and a late decline in clinical parameters. We hypothesise that this inappropriate tissue formation mainly results from suboptimal scaffolds, and that an ideal biomaterial candidate for scaffolds should guide accurate matrix deposition by its structure. In addition, it should provide a protective environment until articular cartilage tissue is rebuilt. In fact, biomaterials currently in use for cartilage tissue engineering often have a random architecture, are soft and prone to deformation by cells or load [23,24]. Therefore, there is an urgent need for a biomaterial that retains its shape during the vulnerable phase of regeneration and supports the formation of adequate matrix by structural, compositional and biomechanical cues.

In search for such materials, obviously, articular cartilage itself has the most natural properties in terms of mechanical behaviour and composition. However, autologous transplants bear the disadvantages of donor site morbidity and limited availability, while vital allografts are also restrictedly available. Decellularised allografts offer a promising alternative, however, the repopulation with host cells has been found challenging, as the exceptionally dense cartilage matrix restricts cellular ingrowth to outer regions [25-27]. Removal of GAG did not result in sufficient porosity to repopulate the matrix thoroughly [28]. Approaches to achieve matrix accessibility by physical perforation involved manual channel piercing with a needle or incising by razor blades [29-31]. However, all these processes remain rather laborious, difficult to standardise or scale-up and do not seem feasible for clinical routine implementation.

For this reason, we hereby propose a concept for an automatised approach of scaffold preparation, by using laser engraving to create fine, well-defined structures into native cartilage. This process can be performed with high precision and in a standardised fashion with consistent quality and allows for large-scale production of an off-the-shelf implant. While being widely used in industry for cutting, welding and engraving, also medical applications for $CO_2$ lasers have been established in various fields, such as dermatology [32], gynaecology [33], dentistry and oral surgery [34,35] with hard and soft tissue applications. Clinical applications for cartilage focus on auricular cartilage and involve ablation of the perichondrium, incisions or targeted deformation of the tissue for otoplasty [36,37]. Recent experimental studies involving $CO_2$-lasered meniscal [38], temporomandibular [39] tracheal [40] and first attempt for articular cartilage [41] show promising results, mainly with porcine and rabbit cartilage. A concept of vital laser-engraved human articular cartilage as allograft has been demonstrated by ProChondrix® (Allosource, Colorado, United States), using laser engravings to facilitate cryopreservation and cell outgrowth. The advantage of this material is the natural content of growth factors incorporated inside the matrix [42]. However, since the availability of allogenic material is restricted and the quality dependent on the donor, a decellularised homologous matrix might be a valuable alternative.

In this study, we aimed to develop a $CO_2$-lasered allogenic cartilage scaffold with reproducible engraving patterns, featuring a maximum amount of deep incisions for accessing even deep scaffold regions with little impact on matrix stiffness. This approach should provide a biomaterial amenable to an off-the-shelf supply, scalable production, and should have good handling properties to facilitate application by the surgeon to maximise long-term benefits for the patients.

## 2. Methods

### 2.1. Sample harvest

Macroscopically intact human articular cartilage was harvested from femoral heads of donors undergoing femoral head replacement, with the approval of the local ethical board and written personal informed consent. Full-thickness non-calcified cartilage was separated from the subchondral bone and biopsies of 8 mm in diameter were prepared with a circular biopsy punch. These biopsies (discs)

were washed with and stored in phosphate-buffered saline (PBS, without $Ca^{2+}/Mg^{2+}$, BE17-512F, Lonza, Switzerland) plus Gentamycin (15710049, Gibco, United States) and Amphotericin B (15290018, Gibco, United States). Sample thickness standardisation was performed with a Teixido cartilage cutter (MicroFrance® by Integra LifeSciences, United States) for 400 $\mu$m thick samples or a self-made cartilage cutting device for 600 $\mu$m or 1 mm thickness. Therefore, the cartilage discs were cut off the deep zone-side, leaving the superficial layer intact.

### 2.2. Laser engraving

A first approach aimed to determine whether $CO_2$ laser engraving was a feasible method to generate structures of the desired dimension (large enough for reseeding but as small as possible; between 30 and 100 $\mu$m) and distribution (as narrow as possible for regular distribution of cells and nutrition of the cartilage matrix, but still providing enough stability) for cellular repopulation and estimate the impact of thermal ablation on the residual cartilage matrix. Holes were engraved into cartilage discs using a Trotec Speedy 300 (Trotec Ltd, Austria) with a standard wavelength of 10.6 $\mu$m, a power of 30 W and a pulse frequency of 5000 Hz. They were lasered with a speed of 42.6 cm/s and three runs in 600 $\mu$m thick cartilage, drawn either with a diameter of 10 or 100 $\mu$m (at least three discs per group). Effects on the cartilage matrix were evaluated via collagen type II immunostaining.

To increase flexibility and cell/scaffold ratio, the holes were then replaced by a grid pattern. To determine the minimal line spacing (since overlap of the V-shaped incision would lead to cutting off the surface) and maximum incision depth, parallel lines were engraved 300 $\mu$m, 500 $\mu$m or 1 mm apart. Full thickness cartilage was used (at least three discs per group) in order to be able to experiment with engraving depth without risking sample disintegration. The speed was again set to 42.6 cm/s, runs ranged from one to nine. The incision shape and the effects of the laser on the matrix were evaluated via collagen type II immunostaining.

In order to achieve a grid incision pattern for the final scaffold design, the line pattern was repeated in a 90° angle. Those scaffolds were imaged with $\mu$CT and used for cell seeding, differentiation and *in vivo* performance experiments.

### 2.3. Matrix pretreatment: devitalisation/decellularisation

Cartilage discs with laser-engraved patterns were either devitalised (mortification of cells) or decellularised (removal of cells and cell remnants, “decell”) with subsequent glycosaminoglycan (GAG) depletion (“decell-deGAG”) as previously developed [28].

For devitalisation, four freeze/thaw cycles (−20 °C / room temperature) were performed, twice frozen dryly and twice frozen submerged in hypotonic buffer (10 mM Tris-base, H5131, Promega, United States, adjusted to pH 8.0 using HCl, K025.1, Roth, Switzerland). Decell-deGAG samples were also subjected to freeze/thaw cycles and then incubated overnight in hydrochloric acid (0.1 M, K025.1, Roth, Switzerland) for decellularisation followed by overnight pepsin treatment (1 mg/mL, P7012, Sigma-Aldrich, United States, in 0.5 M acetic acid, Merck, Germany) for selective matrix depletion. Finally, samples were subjected to a 6 h incubation in sodium hydroxide (0.1 M, 3738.1, Fluka/Sigma, United States). All incubation steps took place under continuous shaking at 180 rpm and 37 °C.

### 2.4. Mechanical compression test

Cartilage discs 1 mm in thickness, engraved within nine runs, were subjected to mechanical compression analysis at different states of preparation: without matrix pretreatment and after decell-deGAG treatment. Native human articular cartilage and three commercially available scaffolds – Chondro-Gide® (Geistlich, Switzerland), TissuFleece™ (Baxter, United States) and Hyalograft™ (FIDIA Advanced Biopolymers, Italy) - were tested for comparison. All samples, at least five per group, were punched to 8 mm diameter and tested under the same conditions.

Mechanical compression was performed on a custom-made compression set fitted on a Zwick BZ2.5/TN1S uniaxial testing machine (Zwick GmbH & Co. KG, Germany) equipped with a 50 N load cell. Before testing specimens were equilibrated in PBS for at least 24 h and then placed inside a well of matching dimensions to mimic the situation in the defect. After achieving a preload of 50 mN, data were recorded and the samples compressed until 80% deformation with a constant speed of 100 $\mu$m per minute. Compressive modulus was calculated between 17 and 20% deformation.

### 2.5. $\mu$CT imaging

Laser-engraved devitalised as well as cell-seeded decellularised and decell-deGAG scaffolds were prepared for $\mu$CT to evaluate the grid pattern in a three-dimensional manner as well as visualise neotissue integration within the crossed line incision. Samples were fixed with 2.5% glutaraldehyde (49630, Sigma Aldrich, United States), rinsed in 0.1 M sodium cacodylate buffer (12300, Electron Microscopy Sciences, United States) and post-fixed with 1% osmium tetroxide (7436.1, Roth, Germany) and 0.07% ruthenium hexammine trichloride (262005, Sigma Aldrich, United States). Then, samples were rinsed and dehydrated in a graded series of alcohol and dried with hexamethyldisilazane (440191, Sigma Aldrich, United States). CT scans of the stained cartilage samples were performed using a SCANCO $\mu$CT 50 (SCANCO Medical AG, Switzerland). Samples were scanned with 90 kVp, 88 $\mu$A, 1500 projections, 600 ms integration time and averaging 3 resulting in a resolution of 2 $\mu$m per voxel.

### 2.6. Ethics of cell donors and animals

ASC were obtained from liposuction material with the written approval of the ethical board of Upper Austria in 2014 (without a reference number) and collected on the base of a written personal informed consent.

Human articular chondrocytes (hAC) were gained with the approval of the local ethical board of the hospital of the Austrian Workers' Compensation Board (AUVA EK 1/2005) and written personal informed consent, from patients undergoing femoral head replacement.

Prior to the animal study, the experimental protocols were approved (GZ: 982788/2015/13) by the City Government of Vienna (municipal authorities MA 58 & 60) in accordance with the Austrian law and the Guide for the Care and Use of Laboratory Animals as defined by the National Institute of Health (revised 2011).

### 2.7. Cell culture

Human adipose-derived stromal/stem cells (ASC) as alternative cell source for cartilage regeneration were used for the *in vitro* adherence and differentiation experiments. ASC were, isolated from liposuction material via collagenase digestion (Collagenase NB4, S1745403, Nordmark, Germany) as described previously [43]. ASC were cultured at 37 °C and 5% $CO_2$ in our standard proliferation medium (EGM-2, CC-3162, Lonza, Switzerland), which has been tested before to retain the chondrogenic potential (unpublished lab-internal standardisation tests). Medium was replaced twice per week and cells were passaged at 70% confluence. In passage three, ASC were harvested via trypsinisation and used for reseeding experiments.

For the *in vivo* experiment, immortalised human ASC (ASC/TERT1, Evercyte GmbH, Austria), characterised in Wolbank et al. [44] were used in order to avoid donor and passage variability. They were expanded in the same way as the primary cells and passaged at 70% confluence.

Bovine articular chondrocytes (bAC) used in the *in vivo* experiment were gained from the femoral condyles and tibia plateau of adult cows obtained from the local abattoir. The cells were isolated via overnight incubation in collagenase (0.15%, 17101-015, Gibco, United States, in DMEM, Gibco). They were cultivated in expansion medium (DMEM, 41966-052, Gibco, United States, supplemented with 10% FCS, P30-3302P+, PAN-Biotech, Germany, 50 $\mu$g/mL ascorbate 2-phosphate, 49752, Sigma-Aldrich, United States, 10 mM HEPES, 15630106, Gibco, 5 $\mu$g/mL insulin, I6634, Sigma-Aldrich, 2 mM L-glutamine, BE17-605E, Lonza, 2 $\mu$g/mL Amphotericin B and 100 $\mu$g/mL Gentamycin) overnight and used one day after isolation.

Human articular chondrocytes were gained from femoral heads of five donors (two female and three male) with a mean age of 55 years. Human chondrocytes were isolated via 1 h incubation in hyaluronidase solution (0.1%, H3506, Sigma-Aldrich, United States in DMEM, 41966-052, Gibco, United States), 0.5 h in pronase solution (10165913103, 0.1%, Roche Switzerland in DMEM) and overnight incubation in a collagenase/papain mix (200 U/mL collagenase, 17101-015, Gibco, United States, and 1 U/mL papain, P4762, Sigma-Aldrich, United States, in DMEM), then cultivated in expansion medium (DMEM supplemented with 10% FCS, 50 $\mu$g/mL ascorbate 2-phosphate, 10 mM HEPES, 5 $\mu$g/mL insulin, 2 mM L-glutamine, 2 $\mu$g/mL Amphotericin B and 100 $\mu$g/mL Gentamycin). Cells were cryopreserved in P0, thawed before the experiment and allowed to adapt to culture for four days at 37 °C and 5% $CO_2$, before seeding onto the scaffolds. Cells of the five donors were pooled in order to reduce donor variability and allow for a small animal group (according to the 3Rs) in this very first animal experiment.

### 2.8. Cell adhesion on cartilage matrix with hole-shaped incisions

To test the cytocompatibility and reseeding efficacy of the laser hole scaffolds, cartilage discs of 600 $\mu$m thickness were engraved with the two dimensions of hole patterns (10 and 100 $\mu$m laser-engraved diameter) and either devitalised or decell-deGAG-treated. Then, the scaffolds (three per group) were transferred to 1.5 mL screw-cap vials and preincubated in DMEM +20% fetal calf serum at 37 °C for 2 h. Each sample was seeded with $1*10^6$ ASC in 1 mL EGM-2 and incubated at 37 °C under continuous rotation of 60 rpm for the whole cultivation period. Medium was replaced three times per week. Samples were harvested after one week and subjected to histological examination.

### 2.9. Cell adhesion and differentiation on cartilage matrix with crossed line incisions

To test for cytocompatibility and cell adhesion of the laser grid scaffold, cartilage discs of 400 $\mu$m thickness with engraved grid patterns (three runs), were either devitalised or decell-deGAG-treated and then transferred to 1.5 mL screw-cap vials and preincubated in DMEM +20% fetal calf serum at 37 °C for 2 h. Three samples were seeded with $1*10^6$ ASC in 1 mL EGM-2 and incubated at 37 °C under continuous rotation of 60 rpm for the whole cultivation period. Medium was replaced three times per week. After one week, medium was switched to chondrogenic differentiation medium, with a low dose of growth factors of 1 ng/mL BMP-6 and TGF$\beta$3 (507-BP and 243-B3, both by R&D systems, United States), respectively (low-dose differentiation medium), for two weeks. Samples were harvested three weeks after reseeding. Presence of vital cells on the scaffolds was examined via Calcein-AM staining (C3099, Thermo Fisher Scientific, United States), adhesion to the scaffold was observed histologically via AZAN staining and $\mu$CT.

For *in vitro* differentiation tests, three decell-deGAG scaffolds of 400 $\mu$m thickness with engraved grid patterns (three runs) were preincubated in DMEM +20% FCS and seeded with $1*10^6$ ASC in EGM-2 per sample. Cultivation took place under continuous rotation at 60 rpm and 37°C during the first 3 days after reseeding, then samples were cultivated statically at 37 °C and 5% $CO_2$. Medium was changed three times per week. One week after reseeding, the medium was switched to differentiation medium supplemented with 10 ng/mL BMP-6 and TGF$\beta$3. Samples were harvested five weeks after reseeding (4 weeks after switching to differentiation medium) and subjected to histological examination.

### 2.10. In vivo *cultivation in an osteochondral plug model*

To examine the performance of CartiScaff *in vivo* in a cartilage defect environment, reseeded scaffolds were implanted into experimental cartilage defects in osteochondral plugs and kept subcutaneously in nude mice [45].

Therefore, osteochondral plugs of 1 cm in diameter, with a cartilage thickness similar to human knee cartilage, were harvested from the tibial plateau and the femoral condyles of bovine knee joints obtained from the local abattoir. Full thickness cartilage defects were prepared using a 4 mm biopsy punch. In a preliminary experiment, four unseeded scaffolds (decell-deGAG treated cartilage discs) were implanted into the defect and tested in the nude mouse model under the same conditions as hereby described, to check for cell invasion from the plug or host.

Decell-deGAG scaffolds with engraved crossed line incision patterns, 4 mm in diameter and either with a thickness of 600 $\mu$m (engraved with five runs, 500 $\mu$m spacing) or 1 mm (nine runs, 500 $\mu$m spacing), depending on the defect depth, were prepared. Before seeding, they were preincubated in DMEM +20% FCS. Scaffolds were either seeded with $0.25*10^6$ bovine or aged human chondrocytes or human immortalised ASC/TERT1.

Since ASC require the combination of TGFß3 and BMP-6 to commit to the chondrogenic lineage [46], seeding of ASC was performed three weeks before implantation. Seeded scaffolds (nine) were cultivated under continuous rotation, one week in EGM-2 and two weeks in chondrogenic differentiation medium supplemented with 10 ng/mL BMP-6 and TGF$\beta$3. Thereafter, six (out of nine) implants were transferred into the defect and implanted subcutaneously into the nude mouse. The other three implants were subjected to histological examination as control.

Chondrocytes were seeded onto the scaffolds (three with bAC, six with hAC) immediately before implantation. Therefore, 2/3 of the cells were directly delivered to the defects and 1/3 of the cells pipetted onto the scaffolds which was immediately afterwards implanted into the defects. Collagen type I/III scaffolds (Chondro-Gide®) of 4 mm diameter were seeded and implanted in the same way (two with hAC) and served as commercial control. Two empty control defects were used as reference from a previous study. Sample size was chosen according to our previous study with this animal model [45]. The number of controls was low due to the knowledge already generated in previous studies. The presented groups were randomly assigned as part of a larger study, the number of animals necessary for the presented study groups was 9.

The interface of the scaffolds and plugs was covered with fibrin sealant (1502524, ARTISS, Baxter, United States) in order to stabilise the scaffolds in the defect and the plugs were kept submerged in expansion medium overnight at 37 °C and 5% $CO_2$. The day after, plugs were implanted subcutaneously into 10-weeks-old female athymic NMRI nude mice (Naval Medical Research Institute; Charles River, Sulzfeld, Germany). As described previously [45].

After arrival of animals from the breeder, animals were kept for acclimatisation for at least two weeks before intervention. Mice were anaesthetised with isoflurane (2−3%, AbbVie, Austria) and two 1 cm incisions were made paramedian on the left and right side of the back. The osteochondral plugs were placed in subcutaneous skin bags, one on each side of the back. Two different groups were combined within one animal according to a plan prepared in advance. Randomisation was done by the incidental order by which animals were taken out of the cage. The incisions were closed by using 6-0 absorbable monofilament sutures (Monosyn, B Braun, Spain). All mice received 1 mg/kg meloxicam (Metacam®, Boehringer Ingelheim, Germany) orally two hours before surgical intervention and for 4 days (S.I.D.) after the operation to alleviate pain and discomfort. The PI but not the surgeon or the animal care attendant was aware of the groups. Animals were kept in groups of five with a stripe-code on the tail. Persisting inflammation at the implant site or pain were the criteria to exclude animals from the study but no animal had to be excluded. After 6 weeks, the animals were sacrificed by using deep inhalation anaesthesia with isoflurane followed by cervical dislocation. The osteochondral plugs were explanted and subjected to histological examination.

### 2.11. Histological examination

Immediately after harvest, samples were fixed overnight in 4% neutral buffered formalin (P087.3, Roth, Germany), rinsed in water and dehydrated with a graded series of alcohol from 50% to 100% EtOH. For decalcification, osteochondral plugs were immersed in USEDECALC decalcification solution (40-3310-00, Medite, Germany) for five weeks with weekly change of the solution. Before embedding, cartilage discs and the osteochondral plugs were cut in half, infiltrated with xylol (CN80.5, Roth, Germany) and embedded in paraffin. 3−4 $\mu$m thick sections were cut with a rotary microtome (MICROM HM355S by Thermo Fisher Scientific, United States), mounted on a glass slide and deparaffinised. Then sections were stained according to the research question: In order to analyse the distribution of the seeded cells on the scaffolds, sections were subjected to AZAN staining displaying cells in intense red and the collagen matrix in blue. For visualisation of fibre orientation, samples used for standard polarised light microscopy (PLM) were stained with picro sirius red while sections undergoing quantitative polarisation microscopy (qPLM) remained unstained. In order to examine the matrix composition, Alcian blue (0.1% in 3% acetic acid at pH 2.5) was used for glycosaminoglycan detection with haemalaun (T865.3, Roth, Germany) counterstaining staining the cell nuclei. Collagen type I and II was distinguished with immunolabelling (collagen type II clone 2B1.5, MA5-12789, or 6B3, MA513026, both Thermo Fisher Scientific, United States, collagen type I PA126204, Thermo Fisher Scientific, United States) either in separate sections or in a double staining. Macrophages were identified with CD68 immunolabelling (ab125212, Abcam, Great Britain), other immune cells such as lymphocytes, granulocytes or monocytes via CD45 (ab10558, Abcam, Great Britain). Degraded and partially degraded collagen type II was visualised via CTX-II immunostaining (PAA686Hu01, Cloud-clone Corp, United States).

The immunohistochemistry sections were treated with BLOXALL (SP6000, Vector Labs, United States) to block endogenous peroxidase and alkaline phosphatase. Antigen retrieval was performed either with citrate buffer (pH 6) for collagen type I, CTX-II and CD45 or pepsin (pH 2) for collagen type II, CD68 and collagen type I for double staining. The primary antibodies were incubated 1:500 (collagen type I), 1:100 (collagen type II and collagen type I for doublestaining, CD45), 1:700 (CTX-II) or 1:200 (CD68,) for 1 h at room temperature. The polymer labelled secondary antibodies (KL DPVR110HRP, Bright vision poly HRP; VWR, United States, anti-rabbit for collagen type I and KL DPVM110HRP anti-mouse for collagen type II) were incubated for 30 minutes at room temperature followed by the ImmPACT NovaRED™ peroxidase substrate kit (SK-4805, Vector Labs, United States) for development of the colour reaction with the polymer system. Counterstaining war performed with haemalaun (T865.3, Roth, Germany). In the double staining ImmPRESS AP reagent (MP-5402, Vector Labs, United States) was used as secondary antibody to collagen type II and incubated for 30 min at room temperature before detection with Vector red alkaline phosphatase (Red AP) substrate kit (SK-5100, Vector Labs, United States). Images were taken with an E800 Nikon laboratory microscope equipped with a NIS software and first histological analysis and CD68 quantification were done blinded.

### 2.12. Quantitative polarized light microscopy (qPLM)

Paraffin sections were prepared as described for histology, then deparaffinised and analysed without staining. The system consists of a transmitted light microscope, equipped with an interference filter (green) with a circular polariser on the illumination side and a rotating linear polariser and a CCD camera at the detection side [47]. Background correction was performed to ensure uniform illumination. The linear polariser was rotated at 0°, 45°, 90° and 135° with respect to a horizontal reference. By comparing signals from the different angles, the average orientation of the polarisation axis with the greater index of refraction (the slow axis) was determined for each pixel (0.5 $\mu$m) and assigned to a colour range for visualisation.

The horizontal reference was defined as -35° to the sample surface to avoid fibre alignments being close to 0° and 180°, which would give a black/pink noise due to those angles being effectively the same but assigned different colours. Fibre alignment was quantified by sorting the colours into one of nine angle ranges (20° each) via a script using FIJI [48] with the plugin boneJ [49].

### 2.13. Biochemical assays

DNA and GAG content of the scaffolds (400 $\mu$m,r 600 $\mu$m or 1 mm in thickness, 6 scaffolds per group) before and after the decell-deGAG treatment were assessed using the CyQUANT® Cell Proliferation Kit (C7026, LifeTechnologies, United States) and the dimethyl methylene blue (DMMB) assay [50] respectively. Twelve untreated human articular cartilage biopsies served as control.

Samples were digested with papain according to a protocol adapted from Kim et al. [51] For DNA quantification, digested samples were incubated with RNAse (R5125, Sigma Aldrich, United States) for 30 min before adding CyQUANT GR dye. Fluorescence was measured at 480ex/520em on a TECAN Infinite 200 reader (Tecan Group AG, Switzerland) in 96-well plates (Greiner, Austria). Measurements were performed in duplicate and DNA content was calculated using linear regression to a standard curve (DNA sodium salt from calf thymus, D3664, Sigma Aldrich, United States).

For the DMMB assay, digested samples were diluted with PBS-EDTA and dimethyl methylene blue was added, resulting in metachromatic changes in absorbance that were detected at 530 and 590 nm. The GAG content was calculated via linear regression to a chondroitin sulphate standard (C4384, Sigma Aldrich, United States).

### 2.14. Quantification and statistics

The program Graph Pad Prism (version 6) was used for statistical analysis and normal distribution of the data was assessed by Shapiro-Wilk-test. Mechanical compression data of the most relevant groups were compared. Since for one out of four groups the assumption of normally distributed values was rejected, Mann-Whitney-U-Tests were performed. Data were displayed as Scatter plots with mean and standard deviation.

To assess the presence of CD68-positive cells in the different groups cultivated *in vivo*, quantification of the CD68 positive area per

incision for three incisions per scaffold was performed via a script using FIJI [48], which segmented positive and non-positive areas via a colour threshold. Data were displayed as Scatter plots with mean and standard deviation. One of the groups had zero-values only (bone marrow group), therefore a Kruskal- Wallis ANOVA by rank was performed. Since the ANOVA indicates that at least two groups differ significantly from one another ($p<0.05$), pairwise comparisons were performed using Mann-Whitney-U-Tests.

In order to quantify the number of laser incisions bearing differentiated neo-cartilage tissue, each single incision was evaluated. On histological paraffin sections of all six samples per group the number of collagen type II positive incisions was counted and compared with the amount of total incisions and evaluated separately for chondrocytes and ASC.

### 2.15. Data sharing

The raw datasets generated within this study are available on request from the corresponding author.

### 2.16. Role of funders

The funders were not involved in any of the steps of the study (study design, analysis data interpretation) or in the writing of the manuscript.

## 3. Results

Within this study, a $CO_2$ laser was chosen to make dense cartilage matrix accessible for repopulation with cells, which is essential for an application as scaffold for cartilage regeneration. Hole, line and grid patterns were tested and the laser-engraved scaffolds were subjected to either devitalisation or decellularisation and GAG depletion and examined for effects on cell adherence and matrix generation. Scaffolds with engraved grid patterns were finally chosen for follow-up experiments and tested for their mechanical characteristics. The chondrosupportive qualities of laser-engraved decell-deGAG scaffolds were demonstrated *in vitro* and *in vivo* in an osteochondral plug model.

### 3.1. Generation of high precision laser incisions into human cartilage

In a first step, holes of different sizes were engraved into human articular cartilage discs of 600 $\mu$m thickness and subjected to histological examination. Circles lasered with a diameter of 10 $\mu$m resulted in holes of about 100 $\mu$m in diameter due to thermal ablation, and circles of 100 $\mu$m in diameter led to a hole diameter of about 250 $\mu$m. AZAN staining for visualizing intact cartilage matrix in blue, showed an intensely stained red ring of about 10–20 $\mu$m lining the edge of the holes (Fig. 1A, B). Immunohistochemistry of collagen type II revealed that the tissue surrounding the holes was unstained, hence appearing like a halo in the range of 150 $\mu$m (Figs. 1B, S1). Both, the unstained halo and the ring of dense matrix vanished after decellularisation and GAG-depletion (Fig. 1B).

To test for cytocompatibility of the lasered cartilage matrices and the possibility to repopulate holes of different diameters, ASC were seeded onto devitalised (freezing only) or decell-deGAG (devitalised + HCl-pepsin-NaOH) treated scaffolds. All holes of both tested sizes were successfully repopulated, and after one week in culture a loose tissue was formed inside holes of both pretreatments (Fig. 1C). However, on devitalised scaffolds still containing the dense matrix ring, the cells were not directly attached but in a distance to the surface, connected only with few cell protrusions and matrix fibres to the surface of the hole. In the decell-deGAG pretreated cartilage samples lacking the dense matrix ring, cells adhered closely to the surface of the hole and also had access to the very superficial empty lacunae fusing with the hole. On the decell-deGAG treated matrix, cells appeared more polygonal and roundish and less spindle-shaped than on only devitalised tissue.

### 3.2. Optimisation of cell to scaffold ratio by crossed line incision pattern engraving

To further increase the cell to scaffold ratio and to obtain greater flexibility, the hole-shaped incisions were replaced by a line pattern which was then further adapted to a grid pattern for biomechanical testing and reseeding. Based on the laser parameters for the hole patterning, different settings were tested to determine the minimal possible line spacing and maximum incision depth.

The $CO_2$ laser-engraved V-shaped incisions with an upper width of about 150 to 200 $\mu$m and an angle which was steeper in deeper incisions than in flatter ones. With the chosen laser settings the number of laser-runs was directly proportional to the incision depth, ranging from 100 $\mu$m at one run to 900 $\mu$m at nine runs in 1 mm thick samples (Figs. 2, S2). A spacing of 300 $\mu$m was possible in 400 $\mu$m thick samples while thicker cartilage needed a distance of 500 $\mu$m for incisions without overlap.

The settings established for the line patterns could be transferred to a crossed line (grid) pattern without adaptations, resulting in a maximum of surface area and sample flexibility. The final scaffold featured a highly regular topography with deep incisions (Fig. 3A–C and supplementary video) and was termed CartiScaff. Indeed, ASC did well adhere and fill up the grids as visualised by Calcein-AM staining (Fig. 3D).

When lasered cartilage matrices were decell-deGAG treated, DNA content reduced from 889 +/−151 dry weight to an overall mean of 51 +/−6 ng/mg, of which the 400 $\mu$m thick samples reached 48 +/−10 ng/mg, the 600 $\mu$m thick samples 64 +/−4.4 ng/mg and the 1 mm samples 41 +/−3.8 ng/mg. The GAG content was lowered from 145 +/−15 to a quite constant value of 13 +/−2.1 $\mu$g/mg dry weight in the three scaffold thicknesses (Fig. 4). The surface of the decell-deGAG treated scaffolds appeared wavier and slightly looser and, as the bulk material, was completely deprived of GAG (Fig. S1).

### 3.3. High compressive modulus suggests suitable biomechanical characteristics of CartiScaff

The impact of the engraved grid patterns with and without decell-deGAG treatment on mechanical characteristics was examined in comparison to native cartilage via compression analysis using samples of 1 mm thickness. The strain stress curves (Fig. 5A) showed that untreated cartilage reached the preset maximum load of 800 kPa at 60% deformation while laser-engraved scaffolds deformed 70% until reaching the maximum load. The decell-deGAG procedure caused further loss in stiffness, reaching 80% deformation at a load of 284 +/-26 kPa. Calculated at a physiologically relevant compression of 17–20% deformation, compressive modulus was highest for untreated cartilage (971 +/−138 kPa) while laser-engraved cartilage retained more than half of its native compressive modulus (494 +/−131 kPa) and laser-engraved decell-deGAG cartilage about one-tenth (8.9%; 86 +/−42 kPa). This left the final scaffold, CartiScaff, still more than 14 times stronger than the stiffest of the three tested commercial scaffolds (Chondro-Gide®), featuring a compressive modulus of 6 +/−3 kPa which is 0.6% of the native cartilage (Fig. 4B).

### 3.4. Scaffolds engraved with crossed lines are well suited for cell adhesion and differentiation of ASC

To test CartiScaff in terms of cytocompatibility, adhesion and differentiation experiments, scaffolds were seeded with ASC and analysed after three weeks of cultivation.

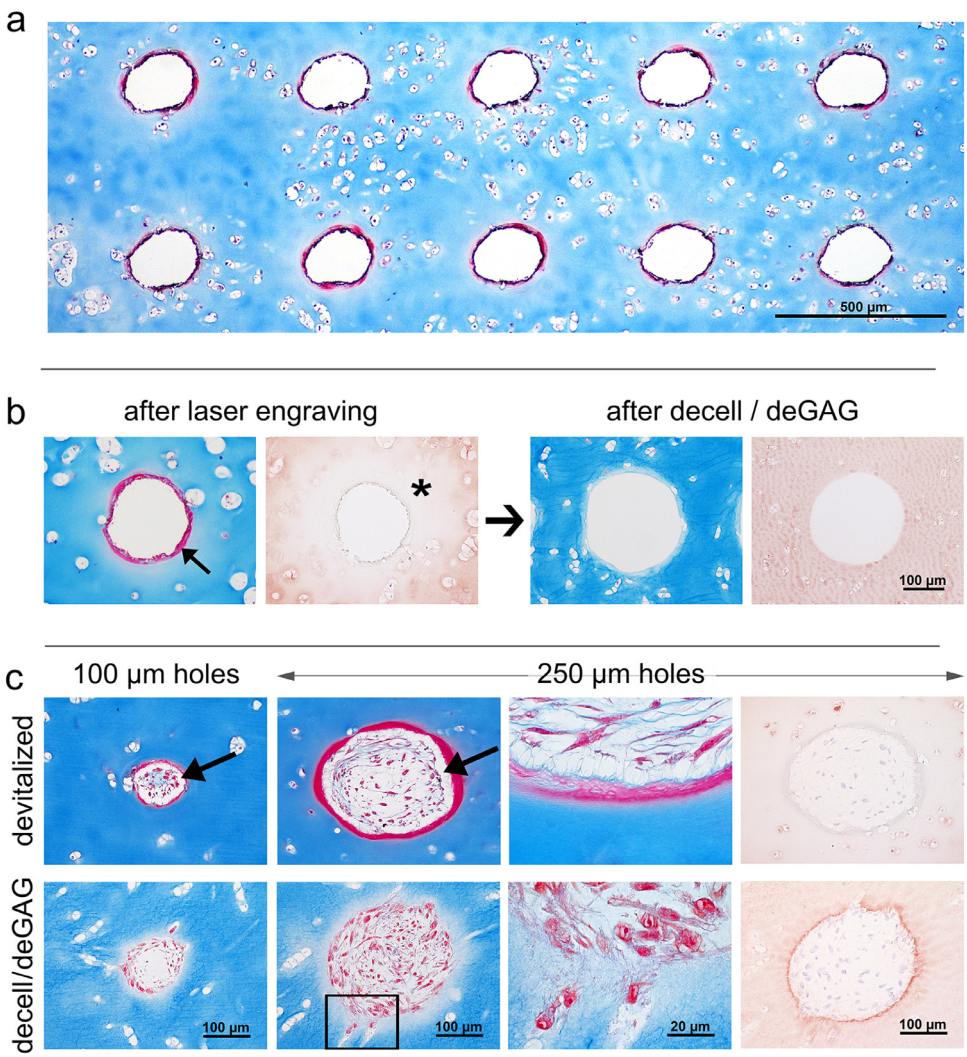


**Fig. 1. Laser-engraved holes: effects on matrix and reseeding.** a) Laser engraving enables the generation of highly regular hole patterns. b) The laser process leads to matrix densification along the edge visible as red ring on AZAN staining (arrow) and altered collagen type II immunoreactivity surrounding the holes (asterisk). Both effects disappeared after decell-deGAG treatment, even though leaving the collagen staining slightly less intense than untreated, unlasered native cartilage ($n > 3$). c) All types of holes (100 $\mu$m, 250 $\mu$m diameter, devitalized, decell-deGAG) are successfully repopulated, yet on devitalized samples cells are in a distance to the densified scaffold surface (arrows) with few fibrous connections (magnification); on decell-deGAG samples repopulation begins at the scaffold border and cells invade accessible lacunae (square and magnification thereof); $n = 3$.

Calcein-AM staining demonstrated ASC to be vital on all samples and present on the scaffold's surface as well as inside the laser-engraved structures (Fig. 3D). Histological examination showed the incisions to be filled with cells and newly deposited matrix after the three weeks culture period in proliferation followed by low dose differentiation medium. Concerning adherence, the same observation as with the seeded holes in Section 3.1 was made on samples with lasered grid patterns. On devitalised scaffolds, neither cells nor the endogenously produced matrix adhered tightly to the scaffold matrix indicated by both histology and $\mu$CT images, which revealed gaps between the newly formed matrix and the scaffold surface (white interspace in histology and black interspace in $\mu$CT; Fig. 6A, B). Even though these gaps are most probably induced by tissue shrinking during dehydration for imaging, it indicates weak bonding of the newly formed tissue. However, on decell-deGAG scaffolds the neo-tissue adhered tightly to the cartilage matrix, and cells invaded empty chondrocyte lacunae that have been made accessible by the laser cut. The collagen fibres of the neo-tissue seemed to merge with the cartilage of the scaffold creating a continuous transition (Fig. 6A). Based on these promising observations, only decell-deGAG scaffolds were included in following reseeding experiments.

To demonstrate *de novo* cartilage formation on CartiScaff (decell-deGAG treated) with engraved crossed line incisions ASC were seeded and cultivated *in vitro* under chondrogenic conditions in the presence of high dose of chondrogenic growth factors (10 ng/mL TGFß3, BMP6). After five weeks, histology showed that grids were filled with a hyaline-like neo-cartilage tissue, staining positive with Alcian blue for GAG and immunostaining for collagen type II (Fig. 6C). This neo-cartilage had intense contact to the scaffold matrix and was well-integrated into the incision. Polarised light microscopy of picro-sirius red stained sections showed the tendency of fibre alignment parallel to the incision surface with a vertical alignment within the incision centre, which is the same orientation as in the scaffold and the native articular cartilage once implanted into a defect (Fig. 6C).

### 3.5. *CartiScaff in an ectopic osteochondral plug model* in vivo *demonstrates regenerative potential*

In order to get a first experience on the performance of the scaffolds combined with cells in an osteochondral environment *in vivo*, the unloaded ectopic nude mouse (NMRI) model was used. Therefore, artificial cartilage defects were generated in bovine osteochondral

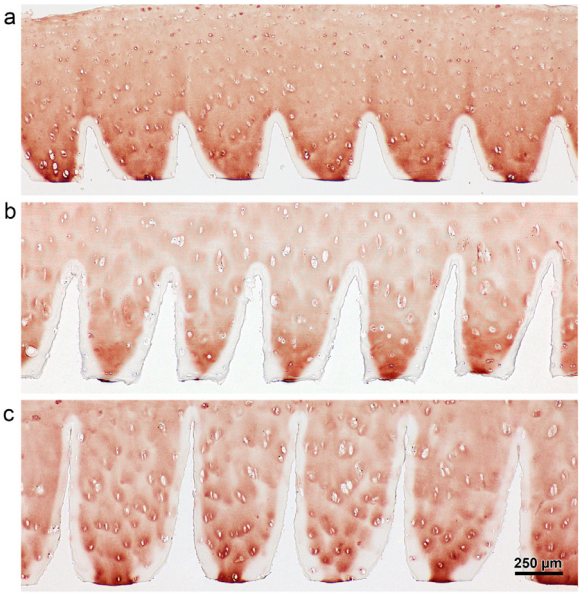


**Fig. 2. Laser-engraved line pattern: direct relation between increasing laser runs and increasing incision depth.** Collagen type II stained cross-sections of cartilage tissue subjected to laser engraving a) 3 runs, b) 6 runs and c) 9 runs. There is hardly any effect on the incision width on surface level or the amount of collagen type II denaturation. $n > 3$.

cylinders, filled with the lasered scaffolds together with either bovine or human chondrocytes or ASC/TERT1 and implanted subcutaneously into the nude mice. Bovine chondrocytes, as cells with a high regeneration potential, were used for a first experiment. In order to represent the clinical situation more closely, in a second *in vivo* experiment, human chondrocytes were chosen as tissue-specific cell type and human ASC/TERT1 as alternative cell source. A commercial collagen type I/III scaffold was used for comparison with a material used in clinics. Scaffolds without cells and empty defects were implanted as controls.

After six weeks *in vivo,* cylinders were recovered and their macroscopic examination suggested no defect filling in controls without scaffold (Fig. 7A), but a completely filled defect with a smooth surface formed by the still intact scaffold (Fig. 7B). A cross-section through

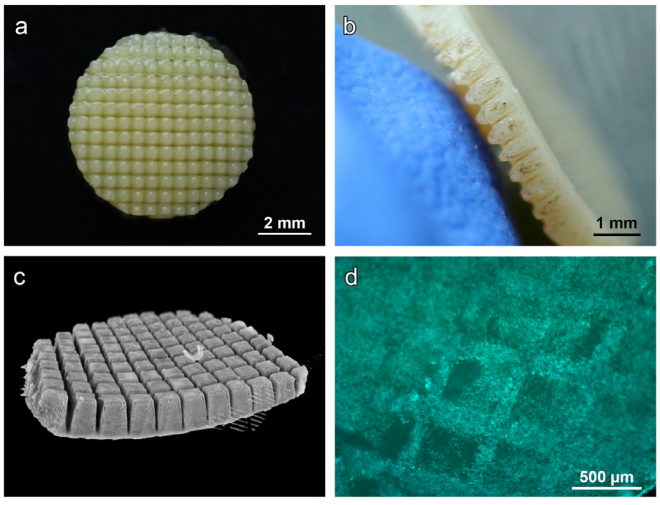


**Fig. 3. Laser-engraved crossed line incisions: spatial appearance.** a) Macroscopic top view and b) side view of cartilage biopsy with laser-engraved cross-wise line incisions and c) $\mu$CT giving a three-dimensional impression of the precise and highly regular grid pattern. d) Calcein-AM staining of ASC seeded on laser-engraved cartilage disc showing a high density of vital cells inside the incisions.

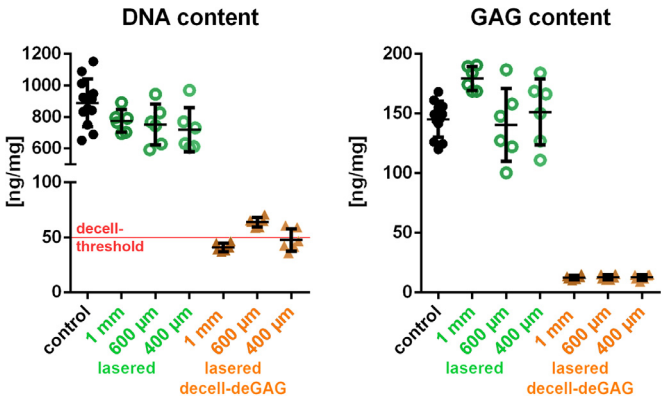


**Fig. 4. DNA and GAG quantification of the laser-engraved, decellularised and GAG-deprived cartilage matrix**. DNA content is reduced from 889+151 to 51+/−6 ng/mg dry weight: to 48+/−10 ng/mg in 400 $\mu$m thick samples, 64+/−4.4 ng/mg in 600 $\mu$m thick samples to 41 +/−3.8 in 1 mm thick samples. GAG content is lowered from 145 +/−15 to 13+2.0 $\mu$g/mg dry weight. Red line at 50 ng/mg in the DNA control marks the threshold of decellularisation. control $n$ = 12; lasered and lasered decell-deGAG samples $n$=6. (For interpretation of the references to colour in this figure legend, the reader is referred to the web version of this article.)

the plug showed the whole depth of the defect to be filled with the scaffold and *de novo* formed tissue (Fig. 7C).

The freshly isolated bovine chondrocytes retained their differentiated character and formed a dense tissue, rich in collagen type II (Fig. 7D) and glycosaminoglycans (Fig. S8). This tissue showed firm integration with the scaffold material – more than with the

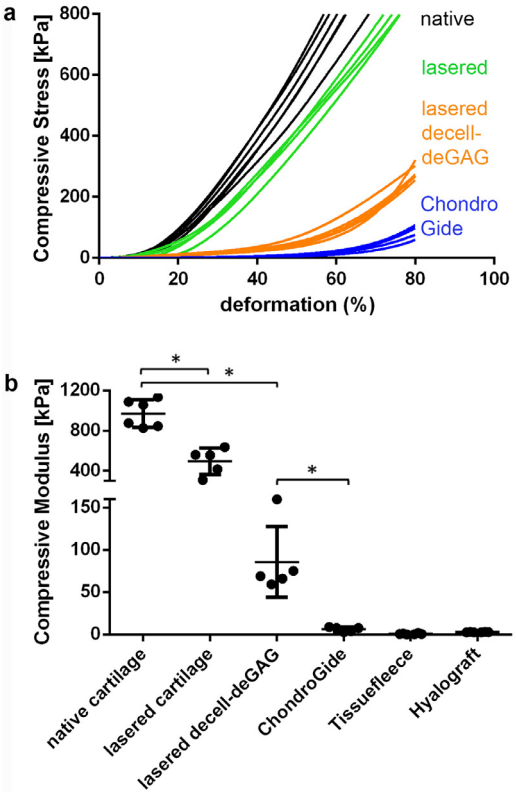


**Fig. 5. Influence of engraved grid patterns and final scaffold pretreatment on compressive stiffness and modulus.** a) Native cartilage reaches 61 +/−4 % and lasered cartilage 74 +/−2 % deformation at the maximal load of 800 kPa while decell-deGAG scaffolds is deformed 80% with 284 +/−26 kPa. 80% ChondroGide-deformation is already reached with 88 +/−20 kPa. b) At 17-20% deformation, compressive modulus of cartilage with laser-engraved grid patterns is reduced to 51% compared to native cartilage. Laser-engraved decell-deGAG cartilage retains 6−16% of its native compressive modulus, leaving it 10 to 26 fold stronger than the commercially available controls; data shown as mean + SD. * $P = 0.05$, $n = \geq 5$ (Mann-Whitney-U-Tests).

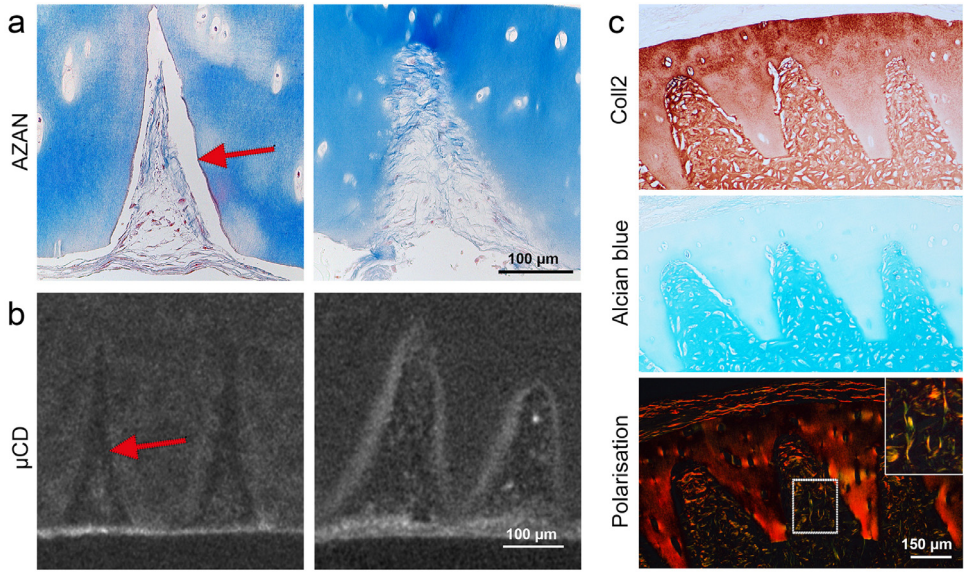


**Fig. 6.** ***In vitro*** **seeding tests on cartilage with laser-engraved grid patterns.** a) AZAN staining and b) $\mu$CT imaging of ASC on laser-engraved cartilage scaffolds after one week of cultivation in proliferation medium followed by two weeks of low dose differentiation medium. On devitalised samples (left) a gap remains between de-novo matrix and the scaffold surface (arrow), while on decell-deGAG treated samples (right) cells adhere tightly to the scaffold matrix. c) After five weeks cultivation of ASC on decell-deGAG treated scaffolds in differentiation medium, (immuno-)histochemistry reveals the presence of neo-cartilage with a dense matrix staining for collagen type II and GAG (Alcian blue) and fully integrated with the scaffold matrix. Polarization light microscopy of picro sirius red stained samples shows collagen fibres aligned along the cutting edges and perpendicular to the cartilage surface (insert). Representative consecutive sections; $n = 3$. (For interpretation of the references to colour in this figure legend, the reader is referred to the web version of this article.)

surrounding cartilage where a gap was visible at the interface to the defect bottom. Despite the scaffold being intact, lacunae in close proximity to the lasered surface were invaded by the bovine chondrocytes surrounded by intensely stained collagen type II (Fig. 7D).

Human chondrocytes were seeded after short *in vitro* expansion of about one week. After six weeks inside the defect they formed a loose tissue, filling the space between scaffold and defect as well as inside the incisions (Figs. 7D, 8A, S4). However,

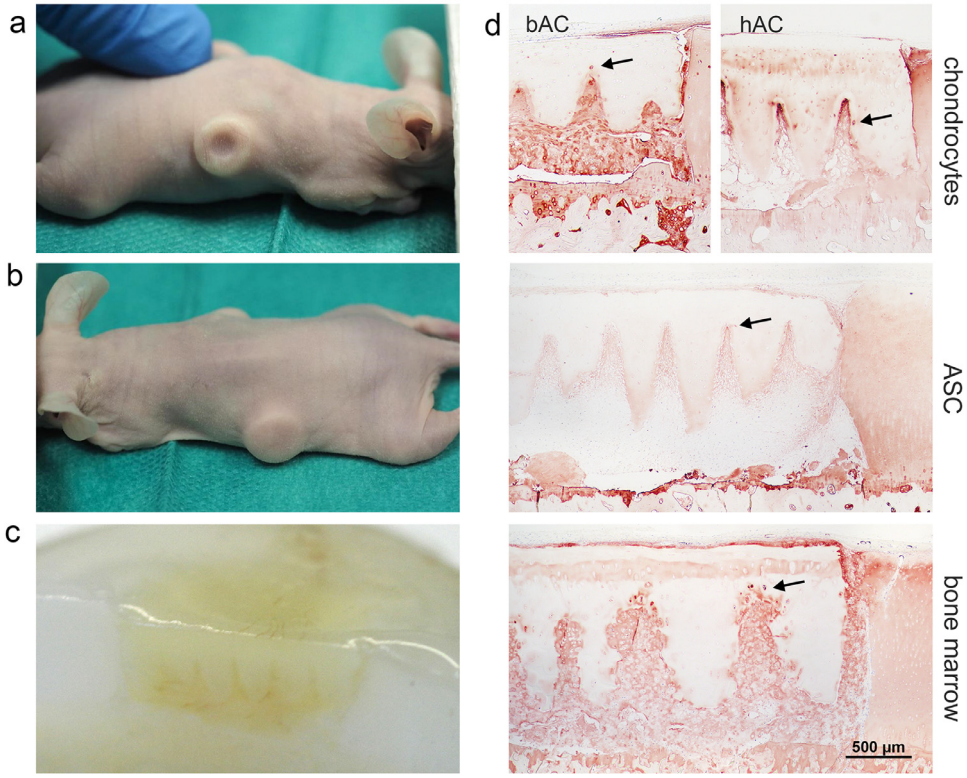


**Fig. 7. Performance of reseeded scaffolds in an osteochondral defect model *in vivo*.** Macroscopic images reveal that after six weeks the experimental defects a) appear to be empty in the control group, while b) defects filled with reseeded scaffolds feature a smooth surface. c) Cross-section through the osteochondral plug proving the filling of the defect with scaffold and new matrix. d) The histological overview sections show the scaffolds and neo-tissue within the defects and differences in distribution of collagen type II. While neo-tissue derived from bovine chondrocytes (bAC) stains regular and intensely, human chondrocytes (hAC) or ASC/TERT1-derived matrix stains strongest within the incisions (tip effect). Bone marrow invading from the subchondral space of the plug forms an intensively stained hyaline tissue all over the defect. The incision edges are more irregular than when chondrocytes or ASC/TERT1 fill the incisions. At some sites collagen type II producing cells are visible inside the scaffold close to the incision edge (arrows). $n = 6$.

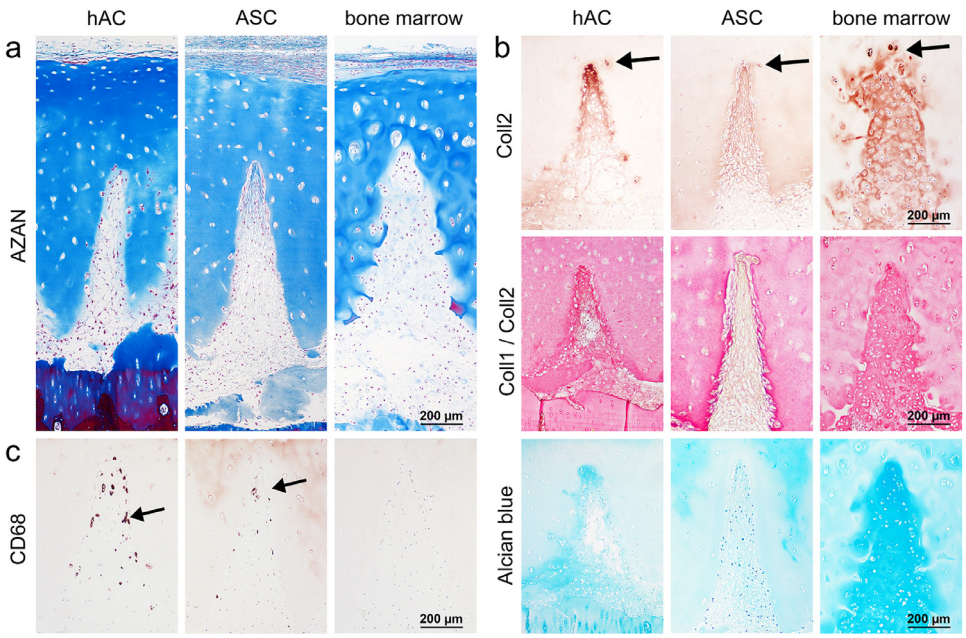


**Fig. 8. Chondrocytes (hAC), ASC/TERT1 or bone marrow cells in the incisions of decell-deGAG treated scaffolds with laser-engraved grid patterns *in vivo*.** (Immuno-)Histochemistry shows a a) regular distribution of cells inside the incisions and b) newly synthesized matrix. Human chondrocyte-derived matrix displays a gradient of increasing staining intensity of collagen type II (Coll2=brown in single-staining) within the incisions (tip effect) and a dominance of collagen type II staining over collagen type I in the double staining (Coll2=pink, Coll1=brown in double-staining). A gradient towards the tip is also visible for GAG in Alcian blue staining. In the ASC/TERT1-seeded scaffolds collagen type II is found along the whole incision with slightly increasing density towards the tip but still generally weaker staining in comparison to the chondrocyte group. Also in the double staining collagen type I is more dominant (brown instead of red in Coll1/Coll2 double staining) and the GAG-staining faint (Alcian blue). Matrix derived from invaded bone marrow cells stains regularly and strong for collagen type II without any visible collagen type I staining (only pink Coll1/Coll2 double staining) and strong GAG (Alcian blue) staining. In all groups some cells invaded empty lacunae inside the scaffold matrix (arrows). c) Staining of CD68 positive cells (arrows) indicates the presence of macrophages in the ASC/TERT1 and hAC group but not in the dense, bone-marrow involving neo-cartilage. $n = 6$. (For interpretation of the references to colour in this figure legend, the reader is referred to the web version of this article.)

inside the incisions the neo-tissue was positive for collagen type II especially along the incision edges, with increasing intensity towards the incision tips, an observation that we term “tip effect” (Figs. 7D, 8B). This phenomenon was found in 52% of all incisions. The hyaline and the fibrous tissue showed good integration with the scaffold and some empty lacunae near the surface were invaded by individual cells (Figs. 7D, 8B).

ASC/TERT1 were precultivated for 3 weeks on the scaffold, two of which in the presence of chondrogenic growth factors. After the three weeks of precultivation, ASC/TERT1 showed no sign of differentiation, when examined by (immuno)histochemistry (Fig. S3). Yet, after six weeks of *in vivo* expansion, similar to the human chondrocytes, collagen type II positive tissue was found inside the incisions (83% of all incisions) with less intense staining than the human chondrocytes but more homogenous distribution inside the incision (Figs. 8B, S4). Overall GAG staining was weak, the matrix appeared more fibrous (Fig. 8A, B) and collagen type I was more dominant (outshining collagen type II in the double staining; Fig. 8B) indicating that the cells were not yet fully chondrogenically differentiated. No morphological signs of osteogeneses (hypertrophy, trabecular structures) were visible.

In the commercial scaffold seeded with human chondrocytes, cells were distributed, yet no collagen type II or GAG stained neo-tissue was visible (Fig. S5). After six weeks in the ectopic *in vivo* setting, the horizontally arranged fibres of the collagen type I/III matrix appeared loose and partially disintegrated.

In the empty control defects there was little fibrous tissue present associated with small interconnections with the subchondral bone, and in one case a hyaline-like cell aggregation, suggesting an origination from bone marrow (preliminary tests, data not shown). Also, in two samples of the reseeded groups, bone marrow appeared to invade from the subchondral space and produced the typical bone-marrow-derived cartilage matrix, with a homogenous appearance, highly positive for collagen type II and GAG and excellent integration with the scaffold (Figs. 7D, 8A, B). The incision edge was substantially degraded and structurally altered in this bone marrow group (Figs. 7D, 8A, B), while degraded collagen type II (CTX-II) within the generally intact matrix was detected in all cell groups, either at the incision edge or around invaded lacuna (Fig. 9). Intact collagen type II was also observed within invading cells and lacunae inside the scaffold (Figs. 7D, 8B).

Since there was obvious bone marrow invasion at least in some samples (Fig. S6), CD68 and CD45 staining were performed to assess

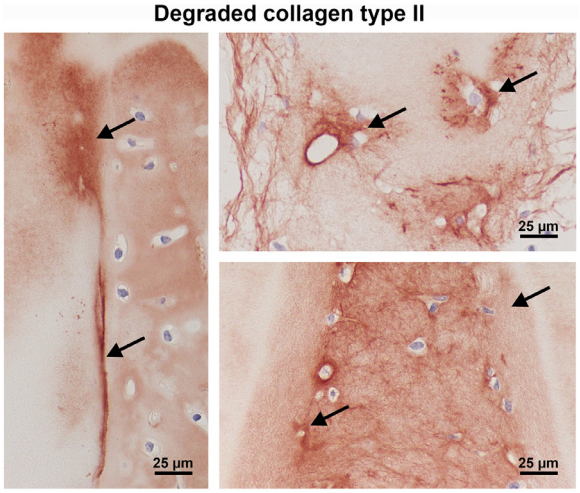


**Fig. 9. Localisation of degraded collagen type II (CTX-II; arrows) at the edge of the scaffold or in the circumference of invading cells.** Incisions of CartiScaff implanted in osteochondral defects with bone marrow (left), hAC (top) and bAC (below) and kept for six weeks *in vivo*.

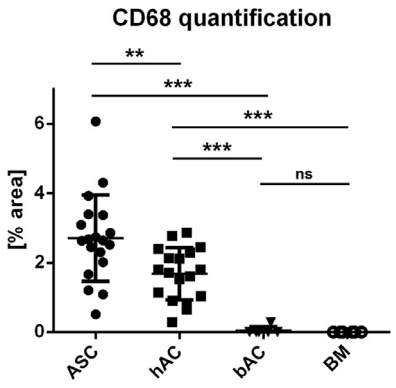


**Fig. 10. Macrophage quantification via CD68 positive areas within the incisions.** Most staining is present in the ASC/TERT1 (ASC) group followed by the hAC group. In bAC only one and in the bone marrow group no incision contains positive areas. data shown as mean + SD. ** $P$ = 0,0036 *** $P$ < 0,0001 (Mann-Whitney U test) ASC/TERT1 $n$ = 19; hAC $n$= 18; bAC $n$= 6; BM $n$= 6.

whether macrophages and leucocytes were present inside the neo tissue. Interestingly, CD45 and especially CD68 positive cells were found in incisions with incomplete chondrogenesis, invading the defect through interruptions in the integrity of the osteochondral interface (Fig. S7), but were absent in the well differentiated neo-cartilage supposedly formed by bone marrow-derived neo-cartilage (Figs. 8C, S7). Quantification of the CD68 positive areas (Fig. 10) underlines this observation, with the area being highest in the ASC/TERT1 group where cells have been shown to be not yet fully differentiated, and lowest in the bovine chondrocyte group and in defects invaded by bone marrow, where collagen type II deposition was most pronounced. qPLM imaging as well as quantitative image analysis demonstrated that the orientation of fibres inside the engraved incisions corresponded well to the orientation inside the scaffold in all groups, with more than half of the fibres being aligned at an angle of 80° to 100° to the scaffold surface, most noticeable in matrix produced by ASC (Fig. 11). The differentiated neo-tissue from bAC did also feature similar orientations as the scaffold matrix in the tip of the incisions. The outer part of the rather small incisions were randomly aligned (Fig. S8).

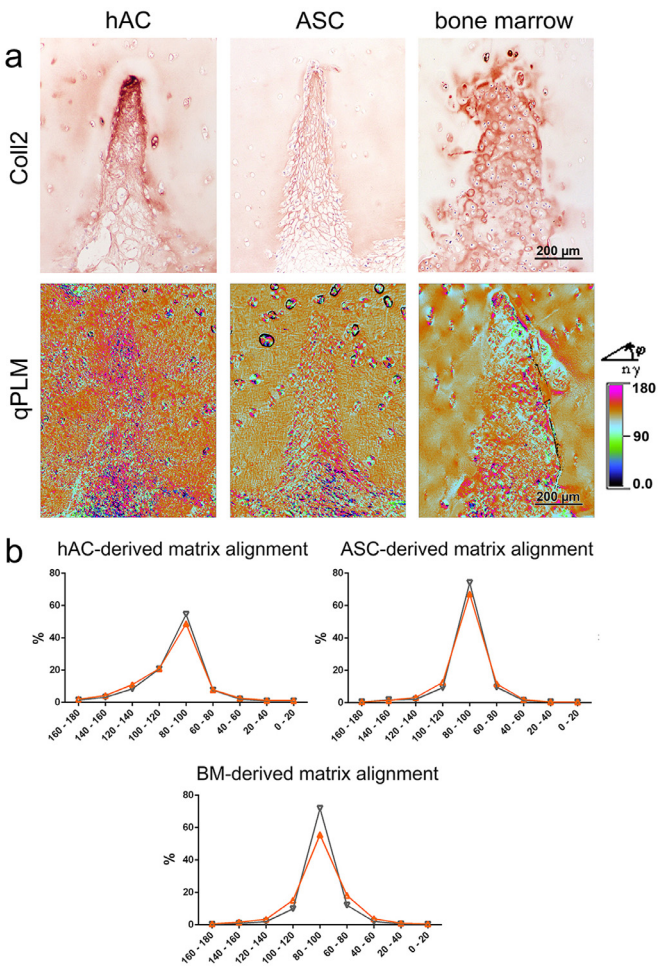


**Fig. 11. Collagen fibre alignment inside the neo-cartilage.** a) Collagen type II staining (same sites as in Fig. 8B) and the corresponding qPLM images, with the fibre orientation for each pixel (0.5 $\mu$m) assigned to a colour range. b) Quantitative distribution of fibre orientation reveals relatively regular fibres alignment inside the engraved incisions (orange curve), corresponding to the alignment inside the scaffold (black curve), both with the majority of fibres arranged in an angle of 80° to 100° to the scaffold surface. BM = bone marrow. (For interpretation of the references to colour in this figure legend, the reader is referred to the web version of this article.)

## 4. Discussion

In this study we demonstrated that the use of a $CO_2$ laser to engrave fine structures into articular cartilage is a suitable method to repopulate decellularised cartilage with therapeutic cells and achieve differentiated neo-tissue, which is well-integrated with the scaffold.

Engineering of the laser-engraved, decellularised scaffolds is precise, allows to preserve the inherent structure of cartilage with its continuous layers (superficial to deep zone), its natural architecture and collagen orientation. The laser technique does not alter the bulk of the cartilage matrix apart from the incision edges and leads to reproducible engravings. Hence, the laser-engraved cartilage scaffold has the potential to permanently or temporarily replace native cartilage in the most appropriate way.

The laser settings tested within this study aimed for the mildest treatment requiring short exposition time, with a short pulse duration and fast laser movement, while still achieving enough power to penetrate the cartilage matrix. Incision depth was determined by the repetition rate. Two types of matrix changes were observed after laser treatment: 1) A narrow dense matrix ring (about 10–20 $\mu$m) with intense staining with azocarmine G (a component of the AZAN stain) lining the surface of the holes and lines. This material most probably derived from condensed matrix residuals resulting from the ablation process and vanished after matrix pretreatment with HCl-pepsin-NaOH and 2) alteration of the matrix in circumference of the laser hole (a halo of about 150 $\mu$m) characterised by the lack of antibody binding in immunohistochemistry against collagen type II. These changes probably result from matrix damage by thermal denaturation (gelatination) of a part of the collagen fibrils [52,53] that hamper antigen accessibility. Interestingly, collagen type II immunoreactivity was restored after matrix pretreatment (decell-deGAG), which might be explained by the removal of damaged matrix masking structurally intact collagen fibrils.

In terms of DNA removal, the decell-deGAG process lowered the DNA content to 48 +/-10 ng/mg in 400 $\mu$m thick scaffolds and 41 +/−3.8 ng/mg in 1 mm thick scaffolds, which complies with the commonly acknowledged threshold of < 50 ng/mg for a scaffold to be termed decellularised [54]. The 600$\mu$m scaffolds remained, with 64 +/−4.4 ng/mg residual DNA, slightly above the threshold. The reason for a lack of correlation between DNA residuals and scaffold thickness could be an unfavourable surface-volume ratio in 600 $\mu$m scaffolds. While 400 $\mu$m scaffolds are generally thin and in the 1 mm scaffold the proportion of the incision is high in relation to the backbone, in the 600 $\mu$m scaffolds the backbone accounts for a higher relative proportion of a quite thick scaffold. To further lower the DNA content of

the 600 $\mu$m scaffolds, either a reduction of the backbone, if mechanically still stable, or an adjustment of the decell-deGAG protocol could be beneficial.

Laser-engraved scaffolds, either devitalised or subjected to decellularisation and GAG depletion, were seeded with ASC to evaluate the influence of the matrix pretreatment on cytocompatibility and cell adhesion. On both, devitalised and decell-deGAG treated laser-engraved scaffolds, cells were viable but adhered stronger to the GAG depleted matrix edges, where new tissue formed a smooth transition to the scaffold matrix. The difference might be related to the dense matrix ring which is not removed in the devitalised scaffolds. It seems to be low-adhesive, either due to a smooth, dense and unstructured surface or the presence of degraded matrix components including GAG which have been shown to have an antiadhesive effect [55,56]. The decell-deGAG process finally removes the dense ring and the remaining cartilage incisions feature enhanced porosity and adhesiveness.

Two main laser patterns, holes and lines or crossed lines (grids) were compared within this study for the beam effect on the matrix, the seeding efficiency and cell-matrix (cell-scaffold) ratio. Compared to holes, the line and grid engraving led to less beam damage on collagen type II (visible as a thinner halo on the collagen type II immunostaining). From a spatial perspective, lines and crossed lines provide more space for new matrix to be generated (higher cell-matrix ratio) and a maximum of surface area, distributing the cells more homogeneously throughout the scaffold. A large surface area was deemed essential, since the seeded cells have to maintain the scaffold matrix, re-load it with GAG or gradually replace it with endogenous matrix. Furthermore, cells perform the transplant integration and are therefore required in sufficient amount at the lateral interface between scaffold and defect. Among the tested patterns, crossed lines provide the most space for cells, especially in comparison with holes, which did not reproducibly stretch through the entire thickness of the scaffold. Moreover, the grid structures produced in this study may further enable better exchange of nutrients through the incisions, which is especially relevant in the first stage after implantation when cells need to adapt to the lowly perfused conditions in the defect. Furthermore, the line and especially the grid structure bears the advantage of making the scaffold more flexible, allowing adaptation to the joint curvatures in larger defects, thus maximizing the scaffold-host contact.

Polarised microscopy of *in vitro* as well as *in vivo* cultivated scaffolds showed the new collagen fibres to have a tendency to align perpendicularly to the cartilage superficial zone, guided by the shape of the engraved incisions. Inside a defect, this corresponds to the natural alignment in articular cartilage. Collagen alignment is of particular relevance for long-term functionality of regenerated articular cartilage since it determines fluid flow within cartilage and substantially contributes to the load bearing capacity of the tissue [21,57]. Therefore, the proper alignment within the neo-cartilage inside the incisions gives rise to the expectation of superior properties of newly synthesised matrix on our scaffold. The guidance of collagen deposition by the engraved incisions is a distinctive feature of CartiScaff and stands in contrast to the structure of the commercial collagen type I/III scaffold, consisting of horizontally aligned fibres that also guide new matrix deposition in this direction. The fibres of the commercial scaffold are further prone to disintegration, already after a short time *in vivo*, forfeiting further support.

Another surprising phenomenon was observed within the incisions: after six weeks *in vivo*, an increased differentiation with obvious collagen type II and GAG deposition was observed within the tips of the incisions (tip effect) in comparison to the wider space and scaffold surrounding. This was the case for human chondrocytes, despite originating from donors above the common age limit of 50 years for MACI [6,58] and despite a previous 2D cultivation step which is known to initiate dedifferentiation of chondrocytes [59,60]. Also ASC, which according to immunohistochemistry showed no indication of collagen type II deposition at the time of implantation, developed this tip effect, indicating that these cells began synthesizing collagen type II inside the incisions *in vivo* without the addition of further growth factors. The staining for collagen type II produced by ASC was less intense than with chondrocytes but more regularly distributed over the incision depth. Obviously, the micro-environment inside the incisions promotes chondrogenic differentiation. Being the most homologous material since produced from cartilage matrix itself, biochemical and biomechanical cues might be responsible for the chondrogenic effect inside the incisions which is supported by studies reporting chondroinductive effects of native cartilage as a whole or distinct cartilage components [61-63] and is topic of further investigations. Moreover, also spatial reasons might have an influence, especially when the newly forming tissue within the tips becomes dense more quickly due to restricted space. This condition probably enhances the chondrogenic stimulus, due to accumulation of endogenous matrix and associated mechanical tension. The tips inside the incisions and the accumulating matrix might also feature an increasingly hypoxic environment, which has been shown to be beneficial for chondrogenic differentiation [64-66] and preservation of the chondrogenic phenotype [67-69].

In addition to the seeded cell types, invasion of the defects and graft by bone marrow-derived cells from the bovine plug occurred in some samples *in vivo*. The hereby created typical bone-marrow derived matrix featured excellent chondrogenic differentiation and integration. While scaffolds in defects without bone marrow invasion showed degraded collagen type II within the matrix, no obvious signs of substantial scaffold matrix degradation were found at the time of explanation. Contrary, bone marrow-derived cells had broken down superficial parts of the scaffold, invaded the empty scaffold lacunae and synthesised new matrix in place. These observations demonstrate that graft remodelling is feasible and that the speed of scaffold degradation and neo-cartilage formation depends on the cell type. Bone marrow is especially adapted to matrix remodelling and is often observed to invade deep cartilage zones from the subchondral plate, with a variety of bone-marrow derived cells such as macrophages and bone-marrow derived mesenchymal stem cells (BMSC) in these areas expressing MMP-1, MMP2, MMP-3 and MMP-13 [70,71]. Immunohistochemical examinations in this study confirmed the presence of macrophages (CD68 positive cells) inside the scaffold incisions. Quantification revealed the highest presence of CD68 positive cells in the ASC/TERT1 and human chondrocyte group, which might be related to the xenogeneic origin of the implanted cells (human cells in bovine osteochondral plugs). However, apart from their xenogeneic origin, ASC/TERT1 and human chondrocytes have also in common that they formed neo-tissue of low density, and not fully differentiated matrix. In fully differentiated sites formed by invading bone marrow or bovine chondrocytes, no macrophages were stained. These observations suggest a transient presence of macrophages, probably due to increasingly inappropriate conditions in the progressively denser neo-cartilage or an adverse effect of the hyaline tissue or chondrocytes [72,73]. However, a controlled study on bone marrow interaction with the lasered cartilage scaffold is necessary to draw conclusions on the fate of bone marrow cells inside the incisions.

The *in vivo* experiments within these studies used the scaffold either pre-seeded (ASC/TERT1) or simultaneously implanted with cells (chondrocytes) and occasionally bone marrow from the plug contributed to tissue formation. This demonstrates that the lasered scaffold is suitable for the three main types of cell-based cartilage treatments: a) classical MACT with a pre-seeded scaffold, b) intraoperative assembly of scaffold with chondrocytes and/or enriched bone marrow from the iliac crest and c) application of scaffold after microfracture. CartiScaff could be easily provided as “off the shelf” product and hence appropriate to replace current clinical materials in an established clinical protocol. However, since bone marrow appears especially promising judging by the few cases of this study, CartiScaff could be particularly favourable for bone marrow-based one-step procedure (e.g. augmented microfracture), and further

improve the already promising results observed in clinical studies [74].

Clinical strategies for scaffold fixation include sutures or the application of adhesives, either alone or in combination. In the unloaded ectopic mouse study fibrin glue was superficially applied for sealing. Fibrin glue is cyto-compatible and comes along with regenerative capacities. It has been shown to serve as biomaterial allowing for chondrocytes as well as mesenchymal stem cells chondrogenesis [75,76]. Nevertheless, its adhesive strength is quite low and might not be sufficient to hold CartiScaff in place under loaded conditions before de-novo tissue has formed. Therefore, an additional fixation might be necessary. We expect that the mechanical stiffness, which is 13 times higher than the tested standard biomaterials currently in use for cartilage regeneration in clinics, has the potential to protect the neocartilage formation from overload and trauma [1,77]. Therefore it might tolerate loading early after surgery and shorten the postoperative physiotherapy [78-81].

The main limitation of our study is that no reliable mechanical data could be gained from *in vivo* samples since the compression analysis was found to be highly influenced by the osteochondral plugs, with great variations between samples (and also between control plugs without a defect). Mechanical testing of in *vitro* cultivated scaffolds cannot be provided since they are often bended by the contractile force of the cells and allover enclosed by newly formed tissue and therefore deemed unrepresentative. Measurements would mainly measure the neo-tissue but not reflect the constrained situation in the joint. In a follow-up study in large animals, alternative mechanical test strategies need to be included.

## 5. Conclusion

Summarised, our approach generating the CartiScaff scaffold with authentic cartilage architecture and zonation and well suited mechanical properties, was shown to support *de novo* synthesis of cartilage matrix *in vitro* and even in an unloaded ectopic animal model *in vivo*. The native structure of the scaffold collagen is preserved and the newly synthesised matrix is guided towards a vertical matrix alignment by the scaffold's topography – an advantage over sponge grafts which promote random matrix deposition. The laser engraved structures greatly increase the cell-scaffold and scaffold-defect contact and promote remodelling. The laser-engraving process can be up-scaled to clinically relevant levels in terms of sample size and throughput. By providing chondrogenic differentiation in the incision tip, improved regeneration can be expected. We believe that decellularised GAG-depleted cartilage with engraved grid-patterns has the potential to efficiently counteract graft failures by preventing early loading damage and improving neo-cartilage formation. Therefore, the newly developed lasered cartilage scaffold holds promises for being beneficial for patients with all current cell- and scaffold-based treatment options. However it first needs verification in orthotopic (large) animal trials.

## Declaration of Competing Interests

Dr. Grillari reports that he is Co-founder and shareholder of Evercyte GmbH, the company providing the ASC/TERT1 cells used in this study. Dr. Nürnberger reports grants from Austrian Research Promotion Agency FFG, grants from Lorenz Böhler Society, during the conduct of the study; In addition, Dr. Nürnberger and Dr. Redl have a patent WO 2018220047 A1 issued. Dr. Redl CEO of Trauma Care Consult. Dr. Heimel and Mrs. Schneider report grants from Austrian Research Promotion Agency FFG grants from Lorenz Böhler Society, during the conduct of the study. Dr. Wolbank reports grants from Österreichische Forschungsförderungsgesellschaft, during the conduct of the study.

## Acknowledgements

This work was funded by the Austrian Research Promotion Agency FFG ("CartiScaff" #842455) as well as the Lorenz Böhler Fonds (16/13) and the City of Vienna Competence Team Project Signaltissue (MA23, #18-08). We further want to acknowledge, Evercyte (Evercyte, Vienna, Austria, Cat# CHS-001-0005) who kindly provided the ASC/TERT1 cell line.

## Contributors

Conceptualisation: SN, HR Funding acquisition: SN, SW, AT; Investigation: SN, CS, BS, CK, PH, XM, MN; Methodology SN, SW, AT; Project administration SN; Supervision SN, SW, HR, AT, PJT; Visualisation: SN, CS, XM, MN; Roles/Writing - original draft SN, CS, CK, PH; Writing - review & editing SN, SW, AT, JG, HR. All authors read and approved the final version of the manuscript.

## Supplementary materials

Supplementary material associated with this article can be found, in the online version, at doi:10.1016/j.ebiom.2020.103196.

## References

[1] Marlovits S, Zeller P, Singer P, Resinger C, Vécsei V. Cartilage repair: generations of autologous chondrocyte transplantation. Eur J Radiol 2006;57:24–31. doi: 10.1016/j.ejrad.2005.08.009.
[2] Brittberg M. Cell carriers as the next generation of cell therapy for cartilage repair: a review of the matrix-induced autologous chondrocyte implantation procedure. Am J Sports Med 2010;38:1259–71. doi: 10.1177/0363546509346395.
[3] Cherubino P, Grassi FA, Bulgheroni P, Ronga M. Autologous chondrocyte implantation using a bilayer collagen membrane: a preliminary report. J Orthop Surg (Hong Kong) 2003;11(1):10–5. doi: 10.1177/230949900301100104.
[4] Aldrian S, Zak L, Wondrasch B, Albrecht C, Stelzeneder B, Binder H, Kovar F, Trattnig S, Marlovits S. Clinical and radiological long-term outcomes after matrix-induced autologous chondrocyte transplantation: a prospective follow-up at a minimum of 10 years. Am J Sports Med 2014;42(11):2680–8. doi: 10.1177/0363546514548160.
[5] Zak L, Albrecht C, Wondrasch B, Widhalm H, Vekszler G, Trattnig S, Marlovits S, Aldrian S. Results 2 years after matrix-associated autologous chondrocyte transplantation using the novocart 3D scaffold: an analysis of clinical and radiological data. Am J Sports Med 2014;42(7):1618–27. doi: 10.1177/0363546514532337.
[6] Marlovits S, Aldrian S, Wondrasch B, Zak L, Albrecht C, Welsch G, Trattnig S. Clinical and radiological outcomes 5 years after matrix-induced autologous chondrocyte implantation in patients with symptomatic, traumatic chondral defects. Am J Sports Med 2012;40:2273–80. doi: 10.1177/0363546512457008.
[7] Filardo G, Kon E, Andriolo L, Di Matteo B, Balboni F, Marcacci M. Clinical profiling in cartilage regeneration: Prognostic factors for midterm results of matrix-assisted autologous chondrocyte transplantation. Am J Sports Med 2014;42:898–905. doi: 10.1177/0363546513518552.
[8] Kon E, Filardo G, Condello V, Collarile M, Martino AD, Zorzi C, Marcacci M. Second-generation autologous chondrocyte implantation results in patients older than 40 years. Am J Sports Med 2011;39:1668–75. doi: 10.1177/0363546511404675.
[9] Filardo G, Kon E, Di Martino A, Patella S, Altadonna G, Balboni F, Bragonzoni L, Visani A, Marcacci M. Second-generation arthroscopic autologous chondrocyte implantation for the treatment of degenerative cartilage lesions. Knee Surg Sports Traumatol Arthrosc 2012;20:1704–13. doi: 10.1007/s00167-011-1732-5.
[10] Wylie JD, Hartley MK, Kapron AL, Aoki SK, Maak TG. Failures and reoperations after matrix-assisted cartilage repair of the knee: a systematic review. Arthroscopy 2016:386–92.
[11] Schuette HB, Kraeutler MJ, McCarty EC. Matrix-assisted autologous chondrocyte transplantation in the knee: a systematic review of mid- to long-term clinical outcomes. Othop J Sports Med 2017.
[12] Bauer S, Khan RJK, Ebert JR, Robertson WB, Breidahl W, Ackland TR, Wood DJ. Knee joint preservation with combined neutralising High Tibial Osteotomy (HTO) and Matrix-induced Autologous Chondrocyte Implantation (MACI) in younger patients with medial knee osteoarthritis: A case series with prospective clinical and MRI follow-up ove. Knee 2012. doi: 10.1016/j.knee.2011.06.005.
[13] Zheng M-H, Willers C, Kirilak L, Yates P, Xu J, Wood D, Shimmin A. Matrix-induced autologous chondrocyte implantation (MACI®): biological and histological assessment. Tissue Eng 2007;13:737–46. doi: 10.1089/ten.2006.0246.
[14] Enea D, Cecconi S, Busilacchi A, Manzotti S, Gesuita R, Gigante A. Matrix-induced autologous chondrocyte implantation (MACI) in the knee. Knee Surg Sports Traumatol Arthrosc 2012;20:862–9.
[15] Zhang Z, Zhong X, Ji H, Tang Z, Bai J, Yao M, Hou J, Zheng M, Wood DJ, Sun J, Zhou SF, Liu A. Matrix-induced autologous chondrocyte implantation for the treatment

of chondral defects of the knees in Chinese patients. Drug Des Dev Ther 2014;8:2439–48. doi: 10.2147/DDDT.S71356.
[16] Macmull S, Parratt MTR, Bentley G, Skinner Ja, Carrington RWJ, Morris T, Briggs TWR. Autologous chondrocyte implantation in the adolescent knee. Am J Sports Med 2011;39:1723–30. doi: 10.1177/0363546511404202.
[17] DiBartola AC, Everhart JS, Magnussen RA, Carey JL, Brophy RH, Schmitt LC, Flanigan DC. Correlation between histological outcome and surgical cartilage repair technique in the knee: a meta-analysis. Knee 2016:344–9.
[18] Mansfield JC, Mandalia V, Toms A, Winlove CP, Brasselet S. Collagen reorganization in cartilage under strain probed by polarization sensitive second harmonic generation microscopy. J R Soc Interface 2019;16(150):20180611. doi: 10.1098/rsif.2018.0611.
[19] Nürnberger S, Klepal W, Vecsei V, Marlovits S. Ultrastructural insights into the world of cartilage - electron microscopy of articular cartilage. Osteosynth Trauma Care 2006;14:168–80 DOI.
[20] Thambyah A, Broom N. Micro-anatomical response of cartilage-on-bone to compression: mechanisms of deformation within and beyond the directly loaded matrix. J Anat 2006;209(5):611–22. doi: 10.1111/j.1469-7580.2006.00646.x.
[21] Korhonen RK, Julkunen P, Wilson W, Herzog W. Importance of collagen orientation and depth-dependent fixed charge densities of cartilage on mechanical behavior of chondrocytes. J Biomech Eng 2008;130(2):021003. doi: 10.1115/1.2898725.
[22] Nakamachi E, Noma T, Nakahara K, Tomita Y, Morita Y. Multiphoton microscope measurement-based biphasic multiscale analyses of knee joint articular cartilage and chondrocyte by using visco-anisotropic hyperelastic finite element method and smoothed particle hydrodynamics method. Int J Numer Method Biomed Eng 2017;33(11). doi: 10.1002/cnm.2864.
[23] Nuernberger S, Cyran N, Albrecht C, Redl H, Vécsei V, Marlovits S. The influence of scaffold architecture on chondrocyte distribution and behavior in matrix-associated chondrocyte transplantation grafts. Biomaterials 2011;32:1032–40. doi: 10.1016/j.biomaterials.2010.08.100.
[24] Rai V, Dilisio MF, Dietz NE, Agrawal DK. Recent strategies in cartilage repair: a systemic review of the scaffold development and tissue engineering. J Biomed Mater Res A 2017;105(8):2343–54. doi: 10.1002/jbm.a.36087.
[25] Kheir E, Stapleton T, Shaw D, Jin Z, Fisher J, Ingham E. Development and characterization of an acellular porcine cartilage bone matrix for use in tissue engineering. J Biomed Mater Res A 2011;99:283–94. doi: 10.1002/jbm.a.33171.
[26] Elsaesser AF, Bermueller C, Schwarz S, Koerber L, Breiter R, Rotter N. In vitro cytotoxicity and in vivo effects of a decellularized xenogeneic collagen scaffold in nasal cartilage repair. Tissue Eng 2014. doi: 10.1089/ten.tea.2013.0365.
[27] Gelse K, Körber L, Schöne M, Raum K, Koch P, Pachowsky M, Welsch G, Breiter R. Transplantation of chemically processed decellularized meniscal allografts: a pilot sheep study. Cartilage 2017;8:180–90. doi: 10.1177/1947603516646161.
[28] Schneider C, Lehmann J, van Osch GJVM, Hildner F, Teuschl A, Monforte X, Miosga D, Heimel P, Priglinger E, Redl H, Wolbank S, Nürnberger S. Systematic comparison of protocols for the preparation of human articular cartilage for use as scaffold material in cartilage tissue engineering. Tissue Eng Part C: Methods 2016;22:1095–107. doi: 10.1089/ten.tec.2016.0380.
[29] Luo L, Eswaramoorthy R, Mulhall KJ, Kelly DJ. Decellularization of porcine articular cartilage explants and their subsequent repopulation with human chondroprogenitor cells. J Mech Behav Biomed Mater 2015;55:21–31 DOI.
[30] Nordberg RC, Charoenpanich A, Vaughn CE, Griffith EH, Fisher MB, Cole JH, Spang JT, Loboa EG. Enhanced cellular infiltration of human adipose-derived stem cells in allograft menisci using a needle-punch method. J Orthop Surg Res 2016;11. doi: 10.1186/s13018-016-0467-x.
[31] Bardos T, Farkas B, Mezes B, Vancsodi J, Kvell K, Czompoly T, Nemeth P, Bellyei A, Illes T. Osteochondral integration of multiply incised pure cartilage allograft: repair method of focal chondral defects in a porcine model. Am J Sports Med 2009;37(Suppl 1):50S–7S. doi: 10.1177/0363546509350045.
[32] Omi T, Numano K. The role of the $CO_2$ laser and fractional $CO_2$ laser in dermatology. Laser Ther 2014;23:49–60. doi: 10.5978/islsm.14-RE-01.
[33] Gambacciani M, Palacios S. Laser therapy for the restoration of vaginal function. Maturitas 2017;99:10–5. doi: 10.1016/j.maturitas.2017.01.012.
[34] Al-Maliky MA, Frentzen M, Meister J. Laser-assisted prevention of enamel caries: a 10-year review of the literature. Lasers Med Sci 2020;35(1):13–30. doi: 10.1007/s10103-019-02859-5.
[35] Suter VGA, Sjolund S, Bornstein MM. Effect of laser on pain relief and wound healing of recurrent aphthous stomatitis: a systematic review. Lasers Med Sci 2017;32(4):953–63. doi: 10.1007/s10103-017-2184-z.
[36] Ragab A. Carbon dioxide laser-assisted cartilage reshaping otoplasty: a new technique for prominent ears. Laryngoscope 2010;120(7):1312–8. doi: 10.1002/lary.20951.
[37] Hsiao YC, Ting K, Su YL, Chang CJ. Continuous cooling system in conjunction with laser surgery for ear reshaping. Lasers Med Sci 2019. doi: 10.1007/s10103-019-02831-3.
[38] Lakes EH, Matuska AM, McFetridge PS, Allen KD. Mechanical integrity of a decellularized and laser drilled medial meniscus. J Biomech Eng 2016;138:031006. doi: 10.1115/1.4032381.
[39] Juran CM, Dolwick MF, McFetridge PS. Engineered microporosity: enhancing the early regenerative potential of decellularized temporomandibular joint discs. Tissue Eng 2015;21:829–39. doi: 10.1089/ten.tea.2014.0250.
[40] Xu Y, Li D, Yin Z, He A, Lin M, Jiang G, Song X, Hu X, Liu Y, Wang J, Wang X, Duan L, Zhou G. Tissue-engineered trachea regeneration using decellularized trachea matrix treated with laser micropore technique. Acta Biomater 2017;58:113–21. doi: 10.1016/j.actbio.2017.05.010.
[41] Li Y, Xu Y, Liu Y, Wang Z, Chen W, Duan L, Gu D. Decellularized cartilage matrix scaffolds with laser-machined micropores for cartilage regeneration and articular cartilage repair. Mater Sci Eng C Mater Biol Appl 2019;105:110139. doi: 10.1016/j.msec.2019.110139.
[42] R. Delaney, C. Barrett, P. Stefens, Cartilage Restoration Matrix Contains Growth Factors Necessary for Hyaline Cartilage Regeneration.
[43] Wolbank S, Peterbauer A, Wassermann E, Hennerbichler S, Voglauer R, van Griensven M, Duba HC, Gabriel C, Redl H. Labelling of human adipose-derived stem cells for non-invasive in vivo cell tracking. Cell Tissue Bank 2007;8(3):163–77. doi: 10.1007/s10561-006-9027-7.
[44] Wolbank S, Stadler G, Peterbauer A, Gillich A, Karbiener M, Streubel B, Wieser M, Katinger H, van Griensven M, Redl H, Gabriel C, Grillari J, Grillari-Voglauer R. Telomerase immortalized human amnion- and adipose-derived mesenchymal stem cells: maintenance of differentiation and immunomodulatory characteristics. Tissue Eng 2009;15(7):1843–54. doi: 10.1089/ten.tea.2008.0205.
[45] Nürnberger S, Schneider C, van Osch GVM, Keibl C, Rieder B, Monforte X, Teuschl AH, Mühleder S, Holnthoner W, Schädl B, Gahleitner C, Redl H, Wolbank S. Repopulation of an auricular cartilage scaffold, AuriScaff, perforated with an enzyme combination. Acta Biomater 2019. doi: 10.1016/j.actbio.2018.12.035.
[46] Hennig T, Lorenz H, Thiel A, Goetzke K, Dickhut A, Geiger F, Richter W. Reduced chondrogenic potential of adipose tissue derived stromal cells correlates with an altered TGF$\beta$ receptor and BMP profile and is overcome by BMP-6. J Cell Physiol 2007;211:682–91. doi: 10.1002/jcp.20977.
[47] Kaminsky W, Gunn E, Sours R, Kahr B. Simultaneous false-colour imaging of birefringence, extinction and transmittance at camera speed. J Microsc 2007;228(Pt 2):153–64. doi: 10.1111/j.1365-2818.2007.01841.x.
[48] Schindelin J, Arganda-Carreras I, Frise E, Kaynig V, Longair M, Pietzsch T, Preibisch S, Rueden C, Saalfeld S, Schmid B, Tinevez JY, White DJ, Hartenstein V, Eliceiri K, Tomancak P, Cardona A. Fiji: An open-source platform for biological-image analysis. Nat Methods 2012:676–82.
[49] Doube M, Klosowski MM, Arganda-Carreras I, Cordelières FP, Dougherty RP, Jackson JS, Schmid B, Hutchinson JR, Shefelbine SJ. BoneJ: free and extensible bone image analysis in ImageJ. Bone 2010;47:1076–9. doi: 10.1016/j.bone.2010.08.023.
[50] Farndale RW, Buttle DJ, Barrett AJ. Improved quantitation and discrimination of sulphated glycosaminoglycans by use of dimethylmethylene blue. Biochim Biophys Acta Biochim Biophys Acta 1986;883:173–7. doi: 10.1016/0304-4165(86)90306-5.
[51] Kim YJ, Sah RLY, Doong JYH, Grodzinsky AJ. Fluorometric assay of DNA in cartilage explants using Hoechst 33258. Anal Biochem 1988;174:168–76. doi: 10.1016/0003-2697(88)90532-5.
[52] J. Pearce, S. Thomsen, Rate Process Analysis of Thermal Damage, Optical-Thermal Response of Laser-Irradiated Tissue1995, pp. 561-606.
[53] Welch AJ, Van Gemert MJC. Optical-Thermal Response of Laser-Irradiated Tissue, Optical-Thermal Response of Laser-Irradiated Tissue. 20111–958. doi: 10.1007/978-90-481-8831-4.
[54] Crapo PM, Gilbert TW, Badylak SF. An overview of tissue and whole organ decellularization processes. Biomaterials 2011;32:3233–43. doi: 10.1016/j.biomaterials.2011.01.057.
[55] Bara JJ, Johnson WEB, Caterson B, Roberts S. Articular cartilage glycosaminoglycans inhibit the adhesion of endothelial cells. Connect Tissue Res 2012;53:220–8. doi: 10.3109/03008207.2011.629310.
[56] Hunziker EB, Kapfinger E. Removal of proteoglycans from the surface of defects in articular cartilage transiently enhances coverage by repair cells. J Bone Joint Surg Br 1998;80(1):144–50. doi: 10.1302/0301-620x.80b1.7531.
[57] Quiroga JMP, Wilson W, Ito K, van Donkelaar CC. Relative contribution of articular cartilage's constitutive components to load support depending on strain rate. Biomech Model Mechanobiol 2017;16(1):151–8. doi: 10.1007/s10237-016-0807-0.
[58] Elmali N, Tandoğan R, Demirel M, Bozkurt M, Beyzadeoglu T. Cartilage repair strategies in the knee: a survey of Turkish surgeons. Acta Orthop Traumatol Turc 2016;50:533–8. doi: 10.1016/j.aott.2016.08.011.
[59] Darling EM, Athanasiou KA. Rapid phenotypic changes in passaged articular chondrocyte subpopulations. J Orthop Res 2005;23(2):425–32. doi: 10.1016/j.orthres.2004.08.008.
[60] Benya PD, Shaffer JD. Dedifferentiated chondrocytes reexpress the differentiated collagen phenotype when cultured in agarose gels. Cell 1982;30(1):215–24. doi: 10.1016/0092-8674(82)90027-7.
[61] Chiu LH, Chen SC, Wu KC, Yang CB, Fang CL, Lai WFT, Tsai YH. Differential effect of ECM molecules on re-expression of cartilaginous markers in near quiescent human chondrocytes. J Cell Physiol 2011;226:1981–8. doi: 10.1002/jcp.22530.
[62] Chang CH, Chen CC, Liao CH, Lin FH, Hsu YM, Fang HW. Human acellular cartilage matrix powders as a biological scaffold for cartilage tissue engineering with synovium-derived mesenchymal stem cells. J Biomed Mater Res A 2014;102(7):2248–57. doi: 10.1002/jbm.a.34897.
[63] Chen CC, Liao CH, Wang YH, Hsu YM, Huang SH, Chang CH, Fang HW. Cartilage fragments from osteoarthritic knee promote chondrogenesis of mesenchymal stem cells without exogenous growth factor induction. J Orthop Res 2012;30(3):393–400. doi: 10.1002/jor.21541.
[64] Das R, Jahr H, van Osch GJVM, Farrell E. The role of hypoxia in bone marrow–derived mesenchymal stem cells: considerations for regenerative medicine approaches. Tissue Eng 2010. doi: 10.1089/ten.teb.2009.0296.
[65] Shang J, Liu H, Li J, Zhou Y. Roles of hypoxia during the chondrogenic differentiation of mesenchymal stem cells. Curr Stem Cell Res Ther 2014. doi: 10.2174/1574888X09666131230142459.
[66] Bae HC, Park HJ, Wang SY, Yang HR, Lee MC, Han H-S. Hypoxic condition enhances chondrogenesis in synovium-derived mesenchymal stem cells. Biomat Res (Biomater Res) 2018. doi: 10.1186/s40824-018-0134-x.
[67] Lafont JE, Talma S, Murphy CL. Hypoxia-inducible factor 2$\alpha$ is essential for hypoxic induction of the human articular chondrocyte phenotype. Arthr Rheum 2007. doi: 10.1002/art.22878.

[68] Murphy CL, Thoms BL, Vaghjiani RJ, Lafont JE. HIF-mediated articular chondrocyte function: prospects for cartilage repair. Arthr Res Ther 2009. doi: 10.1186/ar2574.
[69] Kay A, Richardson J, Forsyth NR. Physiological normoxia and chondrogenic potential of chondrocytes. Front Biosci 2011. doi: 10.2741/339.
[70] Shibakawa A, Yudoh K, Masuko-Hongo K, Kato T, Nishioka K, Nakamura H. The role of subchondral bone resorption pits in osteoarthritis: MMP production by cells derived from bone marrow. Osteoarthr Cartil 2005. doi: 10.1016/j.joca.2005.04.010.
[71] Karadag A, Fisher LW. Bone sialoprotein enhances migration of bone marrow stromal cells through matrices by bridging MMP-2 to $\alpha v\beta 3$-integrin. J Bone Miner Res 2006. doi: 10.1359/jbmr.060710.
[72] Fujihara Y, Takato T, Hoshi K. Macrophage-inducing FasL on chondrocytes forms immune privilege in cartilage tissue engineering, enhancing in vivo regeneration. Stem Cells 2014;32(5):1208–19. doi: 10.1002/stem.1636.
[73] Fujihara Y, Takato T, Hoshi K. Immunological response to tissue-engineered cartilage derived from auricular chondrocytes and a PLLA scaffold in transgenic mice. Biomaterials 2010;31(6):1227–34. doi: 10.1016/j.biomaterials.2009.10.053.
[74] Kaiser N, Jakob RP, Pagenstert G, Tannast M, Petek D. Stable clinical long term results after AMIC in the aligned knee. Arch Orthop Trauma Surg 2020. doi: 10.1007/s00402-020-03564-7.
[75] Bachmann B, Spitz S, Schadl B, Teuschl AH, Redl H, Nurnberger S, Ertl P. Stiffness matters: fine-tuned hydrogel elasticity alters chondrogenic redifferentiation. Front Bioeng Biotechnol 2020;8:373. doi: 10.3389/fbioe.2020.00373.
[76] Ho ST, Cool SM, Hui JH, Hutmacher DW. The influence of fibrin based hydrogels on the chondrogenic differentiation of human bone marrow stromal cells. Biomaterials 2010;31(1):38–47. doi: 10.1016/j.biomaterials.2009.09.021.
[77] Angele P, Fritz J, Albrecht D, Koh J, Zellner J. Defect type, localization and marker gene expression determines early adverse events of matrix-associated autologous chondrocyte implantation. Injury 2015;46:S2–9. doi: 10.1016/S0020-1383(15)30012-7.
[78] Gibson AJ, McDonnell S, Price A. Matrix-induced autologous chondrocyte implantation. Oper Tech Orthop 2006;16:262–5.
[79] Ebert JR, Robertson WB, Lloyd DG, Zheng MH, Wood DJ, Ackland T. Traditional vs accelerated approaches to post-operative rehabilitation following matrix-induced autologous chondrocyte implantation (MACI): comparison of clinical, biomechanical and radiographic outcomes. Osteoarthr Cartil 2008;16:1131–40. doi: 10.1016/j.joca.2008.03.010.
[80] Vogt S, Angele P, Arnold M, Brehme K, Cotic M, Haasper C, Hinterwimmer S, Imhoff AB, Petersen W, Salzmann G, Steinwachs M, Venjakob A, Mayr HO. Practice in rehabilitation after cartilage therapy: an expert survey. Arch Orthop Trauma Surg 2013;133:311–20. doi: 10.1007/s00402-012-1662-9.
[81] Wondrasch B, Risberg MA, Zak L, Marlovits S, Aldrian S. Effect of accelerated weightbearing after matrix-associated autologous chondrocyte implantation on the femoral condyle: a prospective, randomized controlled study presenting MRI-based and clinical outcomes after 5 years. Am J Sports Med 2015. doi: 10.1177/0363546514554910.